

1 **The Antimicrobial Peptide Human Beta-Defensin 2 Inhibits Biofilm**
2 **Production of *Pseudomonas aeruginosa* without Compromising**
3 **Metabolic Activity**

4 **Kevin R. Parducho^{1,2}, Brent Beadell¹, Tiffany Ybarra¹, Mabel Bush¹, Erick Escalera¹, Aldo T.**
5 **Trejos, Andy Chieng², Marlon Mendez¹, Chance Anderson¹, Hyunsook Park¹, Yixian Wang²,**
6 **Wuyuan Lu³, and Edith Porter^{1,*}**

7 ¹Department of Biological Sciences and ²Department of Chemistry and Biochemistry, California
8 State University Los Angeles, Los Angeles, CA, USA

9 ³Institute of Human Virology and Department of Biochemistry and Molecular Biology, University of
10 Maryland School of Medicine, Baltimore, MD, USA

11

12 *** Correspondence:**

13 Corresponding Author

14 eporter@calstatela.edu

15

16 **Keywords:** Airways, antimicrobial peptides, biofilm, cystic fibrosis, epithelial cells, innate
17 immunity, mucosa, *Pseudomonas aeruginosa*

18

19 **Abstract**

20 Biofilm production is a key virulence factor that facilitates bacterial colonization on host surfaces and
21 is regulated by complex pathways, including quorum sensing, that also control pigment production,
22 among others. To limit colonization, epithelial cells, as part of the first line of defense, utilize a
23 variety of antimicrobial peptides including defensins. Pore formation is the best investigated
24 mechanism for the bactericidal activity of antimicrobial peptides. Considering the induction of
25 human beta-defensin 2 (HBD2) secretion to the epithelial surface in response to bacteria and the
26 importance of biofilm in microbial infection, we hypothesized that HBD2 has biofilm inhibitory
27 activity. We assessed the viability and biofilm formation of a pyorubin-producing *Pseudomonas*
28 *aeruginosa* strain in the presence and absence of HBD2 in comparison to the highly bactericidal
29 HBD3. At nanomolar concentrations, HBD2 – independent of its chiral state – significantly reduced
30 biofilm formation but not metabolic activity, unlike HBD3, which reduced biofilm and metabolic
31 activity to the same degree. A similar discrepancy between biofilm inhibition and maintenance of
32 metabolic activity was also observed in HBD2 treated *Acinetobacter baumannii*, another Gram-
33 negative bacterium. There was no evidence for HBD2 interference with the regulation of biofilm
34 production. The expression of biofilm-related genes and the extracellular accumulation of pyorubin
35 pigment, another quorum sensing controlled product, did not differ significantly between HBD2
36 treated and control bacteria, and *in silico* modeling did not support direct binding of HBD2 to
37 quorum sensing molecules. However, alterations in the outer membrane protein profile accompanied
38 by surface topology changes, documented by atomic force microscopy, was observed after HBD2

39 treatment. This suggests that HBD2 induces structural changes that interfere with the transport of
40 biofilm precursors into the extracellular space. Taken together, these data support a novel mechanism
41 of biofilm inhibition by nanomolar concentrations of HBD2 that is independent of biofilm regulatory
42 pathways.

43 **Introduction**

44

45 Biofilms are composed of microbial communities encased in a protective layer of self-produced,
46 extracellular polymers. Biofilms are formed on both abiotic and biotic surfaces and play a significant
47 role in a variety of settings such as aquaculture [1], the food industry, and the clinical field as a factor
48 for antimicrobial drug resistance. Biofilms can colonize body surfaces and mechanisms regarding
49 how our bodies prevent biofilm formation are under extensive investigation [2]. In part, biofilms
50 provide tolerance to host immune factors and antibiotics through impeding their diffusion.
51 Furthermore, biofilms enhance bacterial resistance to these factors by altering bacterial metabolism
52 resulting from the decreased oxygen levels in the center of the biofilm mass as well as the
53 acidification of the local microenvironment [2; 3; 4; 5]. The biofilm matrix is primarily composed of
54 exopolysaccharide, proteins, and extracellular DNA and has been particularly well studied in
55 *Pseudomonas aeruginosa*, a ubiquitous, opportunistic, Gram-negative bacterium. The major
56 structural polysaccharides of *P. aeruginosa* biofilms are Pel, which is composed of positively
57 charged amino sugars, and Psl, which is a polymer of glucose, rhamnose, and mannose; and in
58 certain strains, alginate – an anionic polysaccharide [6; 7; 8]. Proteinaceous components of biofilm
59 include type 4 pili and cup fimbriae serving attachment and various proteins that connect matrix
60 components adding strength to the biofilm [9]. Extracellular DNA (eDNA), which is released via cell
61 lysis [10], plays an important role in priming surfaces for the initial adhesion of the bacteria as well
62 as in maintaining the structural integrity of the polysaccharide fibers [3; 6; 11; 12; 13; 14].
63 Multiple regulatory networks govern the complex process of biofilm formation [15], which
64 progresses from initial attachment mediated by the flagella and the production of pili, to
65 downregulation of flagellar genes, upregulation of the production and secretion of matrix
66 components, maturation, and eventual reappearance of flagella and dispersion. For *P. aeruginosa*,
67 biofilm regulation has been well studied and several regulatory systems have been identified
68 including the Las, Rhl, and quinolone quorum sensing systems, the GacA/GacS two-component
69 system, and c-di-GMP controlled pathways. Key quorum sensing molecules for Las, Rhl, and
70 quinolone systems are N-(3-oxododecanoyl)-homoserine lactone (3-oxo-C12-HSL), N-butanoyl-
71 homoserine lactone (C4-HSL), and 2-heptyl-3-hydroxy-4-quinolone (known as *Pseudomonas*
72 Quorum Sensing molecule or PQS), respectively [16; 17]. These overlapping regulatory systems not
73 only control the production of biofilm but also the production of pigment and various other virulence
74 factors [17; 18]. Genes whose expression is modulated during biofilm formation include *flgF*, which
75 encodes for the basal rod in bacterial flagellin, and *pslA*, which is the first gene in the polysaccharide
76 synthesis locus [19; 20].
77 In addition to being able to produce biofilm, *P. aeruginosa* possesses potent virulence factors such
78 as: a type III secretion system, which allows it to directly deliver exotoxins to host cells [21];
79 rhamnolipids, which enable *P. aeruginosa* to disrupt the tight junctions of respiratory epithelia [22];
80 and pigments with diverse functions in metal-chelation, competitive inhibition of other bacteria, and
81 resistance to oxidative stress [23; 24; 25]. All of these virulence factors and resistance mechanisms
82 contribute to *P. aeruginosa* being one of the leading isolates in healthcare-associated pneumonia in
83 intensive care units and chronic lung infection in patients with cystic fibrosis, a genetic disorder
84 characterized by impaired anion transport and increased mucous viscosity [26]. Yet, despite its

85 ubiquity in nature and its prevalence in healthcare-associated infections, *P. aeruginosa* is not known
86 to cause lung infection in healthy adults, suggesting that humans possess effective innate defense
87 mechanisms in the airways against this organism.

88 Antimicrobial peptides (AMPs) are small, highly conserved effector molecules that play a key role in
89 innate immunity [27; 28]. Present in plants, insects, and mammals, most AMPs are between 2 – 5
90 kDa in size and are cationic with varying degrees of hydrophobicity. Upon the detection of microbial
91 components via pattern recognition receptors, AMPs can be synthesized by epithelial cells and
92 myeloid cells as part of the first line of defense against microbes [29; 30; 31; 32; 33]. A wealth of
93 research has been performed on the ability of AMPs to displace cations bound to bacterial
94 membranes, which are rich in either negatively charged lipopolysaccharides or lipoteichoic acids in
95 addition to anionic phospholipids [34]. After binding to bacterial membranes, AMPs can perturb the
96 membrane structure and form pores mediated by hydrophobic and electrostatic forces. In addition to
97 the charge of the membrane, phospholipid species and the presence or absence of cholesterol, which
98 is absent in bacterial membranes, also affect the binding and orientation of AMPs and hence, their
99 pore-forming capabilities [35; 36; 37; 38; 39; 40]. While pore-formation has been a widely studied
100 mechanism of action, an increasing body of research suggests that the antimicrobial activity of AMPs
101 may also depend on other mechanisms – disruption of cell wall synthesis, metabolic activity, ATP
102 and nucleic acid synthesis, and amino acid uptake [33; 41]. Furthermore, certain AMPs interact with
103 the eukaryotic host cells and have immunoregulatory functions in addition to their antimicrobial
104 activity. A notable example is that LL-37 can also: act as a chemotactic agent to recruit other immune
105 cells and modulate cytokine and chemokine expression in host cells, bind bacterial
106 lipopolysaccharide, and dysregulate the expression of genes involved in biofilm formation [42; 43;
107 44; 45; 46]. Other AMPs have also shown multi-functional capabilities, in particular human beta-
108 defensin 2 (HBD2) and 3 (HBD3), which have been proven to possess mechanisms of action that are
109 more complex than simple pore formation and membrane perturbation [47; 48; 49]. In fact, HBD2
110 was the first human beta defensin to demonstrate chemotactic activity [50]. Beta-defensins are
111 characterized by three, antiparallel β -strands stabilized by three conserved disulfide linkages
112 preceded by an α -helical domain near the N-terminus [51; 52; 53]. Although HBD2 and HBD3 share
113 amino acid sequence and some structural similarities, their overall net charge, hydrophobicity, and
114 charge distribution differ significantly (**Table 1**) and may play a role in their unique and distinct
115 mechanisms of action. Expression of HBD2 and HBD3 is low or absent during steady state but both
116 peptides are induced in airway epithelial tissues during infection or inflammation [31; 32; 48; 54].

117 Due to their lasting potency for millions of years and the feasibility of modifying AMP structures,
118 AMPs continue to be in the spotlight as potential antimicrobial agents [33]. The importance of
119 biofilm in the infection process and in their resistance to antimicrobial agents has been recognized,
120 yet there is a lack of drugs that interfere with biofilm. Therefore, knowledge on the structure-function
121 relationships of AMPs, and the effects of AMPs on bacterial biofilm formation may benefit rational
122 engineering and design of novel AMP variants and therapeutic regimens that are effective against
123 microbial biofilms [55]. Considering the induction of HBD2 and HBD3 and their secretion to the
124 epithelial surface in response to bacteria and their products, we hypothesized that HBD2 and HBD3
125 have biofilm inhibitory activity. We discovered that biofilm and metabolic inhibition are
126 proportionally reduced by HBD3 but not by HBD2. At low concentrations, HBD2 inhibits biofilm
127 production, but not metabolic activity. We undertook multiple approaches to delineate the underlying
128 mechanism for the selective biofilm inhibitory effects of HBD2. This research may lead to the
129 identification of novel targets for the engineering of antimicrobials, which, in the era of increasing
130 multi-drug resistance, is of great importance.

132 **Materials and Methods**

133

134 **Antimicrobial peptides**

135 Chemical synthesis and purification of human beta-defensin 2 (HBD2/L-HBD2), its D- form (D-
136 HBD2) comprised entirely of D-amino acids, its linearized mutant (Linear HBD2 with alanine
137 replacing all cysteine residues), and human beta-defensin 3 (HBD3, in L-form) have been described
138 previously [56; 57]. **Table 1** summarizes their physicochemical properties. Stock solutions (500 μ M)
139 were prepared in 0.01% acetic acid and stored at – 20 °C. For experiments, peptides were used as 10-
140 fold concentration in 0.01% acetic acid.

141

142 **Bacterial culture**

143 For this study, a pyorubin-producing *P. aeruginosa* strain (a cystic fibrosis isolate previously
144 obtained from Dr. Michael J. Welsh, University of Iowa, Iowa City) and *A. baumannii* ATCC 19606
145 were used. For each experiment, snap-frozen 18 h cultures in Tryptic Soy Broth (TSB) (Oxoid) were
146 quickly thawed, subcultured into prewarmed TSB (750 μ L into 50 mL), and brought to mid-log
147 growth phase (3 h at 37 °C, 200 rpm). Bacterial cells were then sedimented and washed with 140 mM
148 NaCl by centrifugation for 10 min at 805 \times g in a precooled centrifuge (4 °C), and resuspended in
149 500 μ L 140 mM NaCl. For gene expression analysis, the suspended bacteria were used directly. For
150 all other assays, the concentration of bacteria was first adjusted to 5×10^7 CFU/mL in 140 mM NaCl,
151 and then further diluted as needed.

152

153 **Biofilm quantification**

154 In a round bottom 96-well polystyrene microtiter plate (Costar #3795), 90 μ L mid-logarithmic
155 growth phase bacteria were added to 10 μ L of 10-fold concentrated defensin or 0.01% acetic acid as
156 solvent control to yield the following final assay conditions: 1×10^6 CFU/mL, 10% Mueller-Hinton
157 broth (Oxoid, without cations), and 140 mM NaCl. Samples were incubated for 18 h at 37 °C and
158 biofilms were quantified according to Merritt *et al.* [58]. Briefly, the content of sample wells
159 containing non-adherent bacteria (planktonic and/or dead) was carefully discarded without disturbing
160 the biofilm, and the well walls were rinsed three times with dH₂O (200 μ L/well) followed by addition
161 of 125 μ L of 0.1% crystal violet (Sigma-Aldrich, St. Louis, MO). After 10 min incubation at RT, the
162 crystal violet solution was removed, wells were rinsed three times with dH₂O (200 μ L/well) and air
163 dried for at least 30 min. To solubilize crystal violet bound to biofilm, 200 μ L of 30 % acetic acid
164 was added to each well and after 15 min incubation at RT 125 μ L was transferred to optically clear
165 flat-bottom 96-well polystyrene microtiter plates (Perkin Elmer from Waltham, MA USA).
166 Absorbance was read at 570 nm using a Victor X3 Plate Reader (Perkin Elmer). Wells containing
167 only 125 μ L of 30 % acetic acid were used to subtract baseline absorbance values from samples for
168 analysis.

169

170 **Metabolic activity measurement**

171 Resazurin reduction was employed as a measure of bacterial metabolic activity [59; 60]. Metabolites
172 accumulating during bacterial growth reduce the weakly fluorescent resazurin to the highly
173 fluorescent resorufin. Samples were prepared as described above but with resazurin (Sigma) added to
174 the assay buffer to obtain a final concentration of 0.01% resazurin (w/v). Relative fluorescent units
175 (RFU) were measured every 3 h with a preheated Victor X3 Plate Reader (Perkin Elmer) at 530 nm
176 excitation and 616 nm emission wavelength and a top read.

177

178

179

180 **ATP quantification**

181 ATP concentrations of non-adherent bacteria were determined using the BacTiterGlo kit (Promega),
 182 with ATP standard curves prepared according to the manufacturer's instructions. Bacteria were
 183 prepared and incubated with defensins for 18 h as described for the biofilm assay. Then, the entire
 184 well contents were transferred to a new 96 well plate, thoroughly resuspended, and of this 75 μ L
 185 from each well was transferred to a black 96-well half area plate (Perkin-Elmer). After addition of
 186 75 μ L ATP substrate solution to each well and 5 min mixing on an orbital shaker, luminescence was
 187 quantified with a Victor X3 plate reader. Seventy-five μ L aliquots of serially diluted ATP standard
 188 were treated in the same way.

189

190 **Pyorubin quantification**

191 Pyorubin is a collection of pigments produced by certain *P. aeruginosa* strains including our test
 192 strain. Although its full chemical composition is unknown, it consists of at least two, water-soluble,
 193 red-colored pigments [61]. Pyorubin quantification was based on Hosseiniidoust *et al.* [23]. Briefly,
 194 bacteria were grown for 18 h in 10% Mueller-Hinton and 140 mM NaCl in the presence of 0.125 to 1
 195 μ M of HBD2 or solvent control in final assay volumes of 1 mL in 12-well microtiter plate (non-tissue
 196 culture treated, Costar). After 18 h incubation, well contents were collected and centrifuged at 5,000
 197 \times g for 10 min at 4 °C to remove non-adherent bacteria. Equivolume mixtures of cell free supernatant
 198 (900 μ L) and chloroform (900 μ L) were mixed and centrifuged at 12,000 \times g for 15 min at 4 °C to
 199 separate the aqueous and organic phases and remove cell debris and other molecules. The aqueous
 200 phase containing pyorubin was lyophilized, dissolved in 125 μ L volume of dH₂O. From this, 100
 201 μ L were transferred to a 96-well flat bottom plate (Perkin Elmer) followed by an absorbance reading
 202 at 535 nm using a Victor X3 Plate Reader (Perkin Elmer).

203

204

205 ***In silico* molecular docking studies**

206 The *in silico* modeling of binding between QS molecules and HBD2 was performed using Autodock
 207 Vina (The Scripps Research Institute) through the UCSF Chimera program
 208 (<https://www.cgl.ucsf.edu/chimera/>). LasR receptor (RSCB 3IX3) and HBD2 (RSCB 1FQQ) were
 209 considered as rigid receptors and were docked with *N*-(3-oxododecanoyl) homoserine lactone (3-oxo-
 210 C12-HSL), *N*-butanoyl homoserine lactone (C4-HSL), and 2-heptyl-3-hydroxy-4-quinolone (PQS) as
 211 ligands. Phosphorylcolamine (NEtP) was used as a negative control. Free energy of binding was used
 212 to calculate dissociation constants using equation (1) with R = 0.00198 kcal/(mol K) and T = 37 °C =
 213 310.15 K [62].

$$K_{D,\text{pred}} = e^{(\Delta G_{\text{bind}})/[(R/1000)*T]} \quad (1)$$

214

215

216 **Gene expression analysis**

217 Mid-logarithmic growth phase bacteria were prepared and washed as described above. The assay was
 218 up-scaled using 12-well polystyrene flat bottom plates with non-reversible lids with condensation
 219 rings (Genesee Scientific, San Diego, CA, USA). Twenty μ L of the washed bacteria was added to
 220 HBD2 or solvent (100 μ L of 10-fold concentrated defensin in 0.01% acetic acid or 0.01% acetic
 221 acid, respectively, diluted in 900 μ L 10% Mueller Hinton/140 mM NaCl) yielding about 1×10^8
 222 CFU/mL. After incubation at 37 °C for the specified time points, biofilm and planktonic phase
 223 bacteria were homogenized by 10 min vortexing with 1 mm glass beads and tightly secured lids
 224 (Sigma-Aldrich, St. Louis, MO, USA). RNA extraction was performed on the homogenized samples
 225 using an RNeasy Mini Kit (Qiagen, Hilden, Germany) following the manufacturer's enzymatic lysis
 226 and mechanical disruption protocol with acid-washed 425-600 μ m glass beads (Sigma-Aldrich).
 227 Residual genomic DNA was removed with in-solution TurboDNase treatment (2 U/ μ L, Invitrogen,

228 Carlsbad, CA, USA) according to the manufacturer's recommendations followed by purification and
229 concentration of RNA samples with RNA Clean & Concentrator-5 kit (Zymo Research, Irvin, CA,
230 USA). Purity of RNA was confirmed by lack of amplification in SsoAdvanced™ Universal SYBR®
231 Green (Bio-Rad, Hercules, CA, USA) real-time PCR using the RNA samples as template and primers
232 for the housekeeping gene *gapA* (see **Table 2**). Confirmed pure RNA samples were reverse
233 transcribed with iScript Reverse Transcription Supermix (Bio-Rad) and resulting cDNA was diluted
234 to 25 ng/µL in nuclease free water. SsoAdvanced™ Universal SYBR® Green real-time PCR was
235 performed with target primers for *pslA* and *flgF* and housekeeping gene *gapA* as reference gene (see
236 **Table 2**, used at 0.75 µM final concentrations) in 10 µL reaction volumes and 12.5 ng cDNA input.
237 Primers (Integrated DNA Technology's, IDT, Coralville, IA, USA) were designed using IDT's
238 primerQuest Tool. Quantitative PCR (qPCR) and subsequent melt curve was performed using BIO-
239 RAD's CFX96 Real Time Thermocycler following standard conditions with annealing/extension at
240 60°C. CT values and relative gene expression were determined with BIO-RAD's CFX Maestro
241 Version 1.1. Amplified products were verified through size determination via standard agarose gel
242 electrophoresis and melt curve analysis. Each time point was assessed in three independent
243 experiments conducted in duplicates for a total n of 6. Initially, *16S rRNA* was considered as a second
244 housekeeping gene. However, its CT values (around 5) were substantially earlier than the CT values
245 for the target genes and *gapA* (at or above 20) and thus, *16S rRNA* gene expression was not further
246 evaluated in this study.
247

248 **Outer membrane protein profile analysis**

249 *P. aeruginosa* outer membranes were harvested after incubation with HBD2 or solvent control
250 according to Park et al. 2015 [63] with minor modifications. Briefly, bacteria were prepared as above
251 and then grown for 18 h in 10% Mueller-Hinton and 140 mM NaCl in the presence of 0.125 to 1 µM
252 of HBD2 or solvent control in final assay volumes of 1 mL in 12-well microtiter plate (Costar® not
253 treated, Corning). After 18 h incubation, the well contents were resuspended, transferred into
254 microfuge tubes, and centrifuged at 5,000 × g for 10 min at 4 °C to pellet the bacterial cells. Cells
255 were then resuspended in 80 µL of 0.2 M Tris-HCl, pH 8.0. Then, 120 µL lysis buffer was added to
256 the resuspended cells (final conditions were 200 µg/mL hen egg white lysozyme (Sigma-Aldrich), 20
257 mM sucrose and 0.2 mM EDTA in 0.2 M Tris-HCl, pH 8.0). After a 10 min incubation at RT, 2 µL
258 of Protease Inhibitor Cocktail (Sigma Aldrich P8340) was added followed by 202 µL of extraction
259 buffer (10 µg/mL DNase I [Sigma-Aldrich DN25] in 50 mM Tris-HCl/10 mM MgCl₂/ 2 % Triton
260 X-100). After 1.5 h incubation on a rocker at 4°C, samples were centrifuged at 1500 × g at 4°C for 5
261 min. The resulting supernatants from triplicate samples, which contain the outer membranes, were
262 pooled and placed into 4 mL ultrafiltration tubes with 5 kDa cut off molecular weight (Amicon
263 Ultracel, 5k, Millipore). PBS was added to yield a volume of 4 mL, and then the tubes were
264 centrifuged at 2400 × g until about 500 µL residual volume was obtained. The outer membranes in
265 this residual were then washed by suspending in 3.5 mL PBS and then centrifuging at 2400 × g for 25
266 min at RT, yielding a residual volume of approximately 200 µL. Of this, 4 µL were subjected to
267 standard SDS-PAGE using Bio-Rad 16.5 % Mini-Protean Tris-Tricine gels followed by silver stain.
268 Images were acquired with Versadoc (Bio-Rad) and analyzed with Image Lab version 6.01 software
269 from Bio-Rad Laboratories.
270

271 **Atomic force microscopy**

272 *P. aeruginosa* (1 × 10⁶ CFU/mL inoculum) was incubated in 10 % Mueller Hinton broth/140 mM
273 NaCl/12.5 mM sodium phosphate pH 7.0 with and without HBD2 (0.25 µM), on glass coverslips
274 (Borosilicate glass square coverslips, Fisher Scientific) in 6-well plates (Corning) for 18 h at 37°C.
275 As negative controls for HBD2 the peptide solvent 0.01% acetic acid was included, respectively.

276 Coverslips were then transferred into wells of a fresh 6-well plate and adherent bacteria were fixed
277 with 2.5 % glutaraldehyde (Ted Pella, CA; 0.25% in PBS, electron microscopy grade) for 20 min at 4
278 °C followed by washing with deionized water according to Chao and Zhang, 2011 [64], and stored at
279 4°C until imaging by atomic force microscopy (AFM).

280 All AFM tests [65] were carried out with a NX12 AFM system (Park System) using an aluminum
281 coated PPP NCHR (Park systems) cantilever with a spring constant of 42 N/m, a resonance
282 frequency of 330 kHz, and a nominal tip radius of < 10 nm. At least five images were acquired per
283 sample in air with non-contact mode (NCM) with settings of 256 pixels/line and 0.75 Hz scan rate
284 and continuous monitoring of the tip integrity. The images were first order flattened and the
285 roughness and height of all bacteria were measured using XEI software (Park Systems). Specifically,
286 roughness of each bacterium was calculated from the root mean square value (RMS, i.e. standard
287 deviation of the distribution of height over the whole bacterium surface).

288
289

290 **Data and statistical analysis**

291 Data graphs were generated using Microsoft Excel® 2016 or Graphpad Prism 7.04 Software.
292 Statistical analyses were performed using IBM SPSS version 24 or Graphpad Prism 7.04 Software. A
293 p-value < 0.05 was considered statistically significant.

294
295

296 **Results**

297

298 **At low concentrations, HBD2 does not reduce metabolic activity but inhibits biofilm production 299 by *P. aeruginosa*, unlike HBD3**

300 To compare the antimicrobial activities of HBD2 and HBD3, *P. aeruginosa* was exposed to either
301 peptide at various concentrations over a period of 18 h. Viability was assessed by measuring
302 metabolic activity every 3 h via quantification of resazurin reduction to the highly fluorescent
303 resorufin by bacterial metabolites. Biofilm was assessed at 18 h post-incubation via quantification of
304 crystal violet staining through absorbance readings. The resazurin reduction assay showed that both
305 HBD2 and HBD3 reduced metabolic activity in a dose-dependent manner, with HBD3 being more
306 effective on a per molar basis, producing around a 30% reduction at 0.5 µM compared to the 4 µM
307 needed by HBD2 at 18 h for the same effect (**Figure 1**). However, when comparing the effect on
308 biofilm production between the two peptides, a notable difference was observed. At concentrations of
309 0.25 and 0.5 µM, HBD2 reduced *P. aeruginosa* biofilm to ~ 75% of the control without significantly
310 reducing the metabolic activity (**Figure 2A**). In contrast, at these concentrations, HBD3 reduced the
311 formation of *P. aeruginosa* biofilm in a dose dependent manner that was directly proportional to the
312 cumulative effect on metabolic activity and further reduced both biofilm and resorufin production to
313 nearly undetectable levels at a concentration of 1 µM (**Figure 2B**) consistent with direct microbicidal
314 activity. ATP concentrations measured at the end of the 18 h incubation period corroborated the
315 resazurin data (**Figure 3**), showing maintained ATP levels in HBD2 treated bacteria but a significant
316 reduction of ATP levels in HBD3 treated *P. aeruginosa* (at 2 µM defensin, 17.65 ± 5.31 nM ATP
317 compared to 3.6 ± 2.88 nM ATP, respectively, $p = 0.011$). These data suggest a differential
318 mechanism for the antimicrobial activity between HBD2 and HBD3, and that HBD2 selectively
319 inhibits biofilm formation at low concentrations.

320
321

322 **HBD2 similarly inhibits biofilm production by *A. baumannii* without reducing metabolic 323 activity at lower concentrations**

324 To rule out that the observed differential biofilm reducing activity of HBD2 activity was strain-
325 specific and restricted to *P. aeruginosa*, we also subjected *A. baumannii*-another opportunistic Gram-
326 negative rod of clinical relevance - to varying doses of HBD2 and determined resazurin reduction and
327 biofilm production after 18 h incubation. As shown in **Figure 4**, at low concentrations, HBD2
328 similarly inhibited biofilm formation while not reducing metabolic activity of *A. baumannii*. For
329 example, at 1 μ M, HBD2 effected a significant reduction of biofilm to 51.77 ± 2.93 % of the control
330 ($p < 0.001$) while resazurin reduction was still at 115 ± 0.67 % ($p = 1.0$,) of the control (means \pm S.D.,
331 $n = 3$). At higher concentrations though, HBD2 appeared to have greater effects on *A. baumannii*
332 compared to *P. aeruginosa* as both biofilm and metabolic activity were reduced to less than 2 % and
333 20 % of the control at 4 μ M HBD2, respectively (1.23 ± 0.48 % and 18.71 ± 10.43 %, means \pm S.D.,
334 $n = 3$).

335

336 **HBD2 biofilm inhibitory activity does not depend on chirality but on folding state**

337 Since HBD2 appeared to selectively reduce biofilm formation and it has been known to bind to
338 chemokine receptors on eukaryotic cells [66; 67], it was possible that the effects of HBD2 were due
339 to binding to receptors involved in the biofilm regulatory pathway such as the GacA/GacS system.
340 To test this, we assessed the activity of the D-form of HBD2, which, due to mismatched chirality,
341 does not bind to proteinaceous receptors of L-HBD2. Like L-HBD2, D-HBD2 effected a significant
342 reduction of biofilm production by *P. aeruginosa* without reducing metabolic activity (**Figure 5A**).
343 Thus, this suggests that the observed HBD2 effect on *P. aeruginosa* biofilm production was not due
344 to binding to receptors important for biofilm regulatory pathways.

345 Upon proper folding, defensins form three intramolecular disulfide bridges, which stabilize an
346 amphipathic structure where cationic and hydrophobic amino acid residues are spatially segregated.
347 To assess the importance of the structure and thus, charge distribution of HBD2 for its observed
348 activity, a comparison was made between wildtype HBD2 and a linearized HBD2 mutant (Linear
349 HBD2) with cysteine residues replaced by alanine residues. Loss of the cysteine residues prevents the
350 formation of stabilizing disulfide bonds, drastically limits proper folding, and disrupts the
351 organization of charged domains thought to be critical for AMP activity [68; 69; 70]. As shown in
352 **Figure 5B**, linearization of HBD2 resulted in a pronounced loss of activity.

353 Taken together, these data provided evidence for a receptor-independent activity that requires proper
354 sequestration of charged and hydrophobic residues. We next asked whether HBD2 disrupts
355 regulatory pathways of biofilm production through QS molecule binding. To answer this question,
356 we took a three-pronged approach and performed *in silico* docking studies with known QS molecules
357 involved in biofilm regulation, employed qPCR probing for genes differentially expressed during
358 biofilm formation, and quantified pyorubin, a pigment regulated by the pathways that also affect
359 biofilm production.

360

361 **HBD2 binding to QS molecules is unlikely based on Autodock Vina prediction**

362 QS molecules are small and flexible molecules with a potential for hydrogen bonding and
363 hydrophobic interactions. Thus, they may bind to and be sequestered by HBD2. To explore this
364 further, Autodock Vina was used (**Figure 6**) to predict HBD2 binding to known *P. aeruginosa* QS
365 molecules representing three different QS systems, namely 3-oxo-C12-HSL – as the major QS
366 molecule for *P. aeruginosa* utilized by the Las system, C4-HSL primarily utilized by the Rhl
367 system, and PQS a key sensing molecule in the 4-quinolone system [71]. As a positive control,
368 Autodock Vina was also used to match the known binding pocket of the QS molecule 3-oxo-C12-
369 HSL to its receptor LasR that has been previously assessed by X-ray diffraction (RSCB 3IX3 [72]).
370 Phosphorylcocolamine (NEtP), which is not expected to bind to either LasR receptor or HBD2, was
371 used as a negative control. Using the same methodology that confirmed binding of 3-oxo-C12-HSL

372 to LasR here, (Figure 6A) no binding of 3-oxo-C12-HSL to HBD2 was found (Figure 6B).
373 Furthermore, we calculated the free energy of binding and found for LasR values corresponding to
374 those reported in the literature [62; 73]. Employing a -6 kcal/mol threshold for likely binding
375 between ligand and receptor, binding between LasR and 3-oxo-C12-HSL, C4-HSL, and PQS was
376 much more favorable (Figure 6C) than binding between HBD2 and these sensing molecules (Figure
377 6D).

378 Using equation [1], the dissociation constants (K_D) for the most favorable binding pair between either
379 LasR or HBD2 with each QS molecule was calculated (Table 3). This method predicted the K_D of 3-
380 oxo-C12-HSL and LasR (1.15 μ M) near that of previously reported values (~5.5 μ M) [74].
381 Furthermore, K_D values for LasR binding with all three *P. aeruginosa* QS molecules were
382 consistently two to three orders of magnitude lower than those of HBD2 binding with any of these
383 QS molecules. This suggests that it is unlikely for HBD2 at physiological concentrations [75; 76; 77]
384 to significantly bind these QS molecules.
385

386 **Gene expression of *flgF* and *pslA* is not affected by HBD2**

387 During biofilm formation, motility and production of exopolysaccharide are reciprocally regulated
388 with reduction of the expression of flagella-related genes and increase in the expression of genes
389 contributing to polysaccharide synthesis including PIs polysaccharide. Thus, we compared the
390 expression of *flgF* (Figure 7A) and *pslA* (Figure 7B) in *P. aeruginosa* treated with 0.25 μ M HBD2
391 or solvent at various timepoints for up to 12 h. For solvent treated control bacteria, as expected, *flgF*
392 gene expression decreased within 2 h reaching statistical significance after 6 h and the expression of
393 *pslA* was significantly increased after 2 h compared to the later time points ($p < 0.01$ and $p < 0.05$ in
394 multivariate ANOVA with Bonferroni posthoc analysis). As observed for control bacteria, *flgF* gene
395 expression decreased over time and was significantly reduced in HBD2 treated bacteria ($p < 0.05$)
396 though changes in *pslA* gene expression did not reach statistical significance. However, there was
397 overall no statistical significant difference between solvent and HBD2 treated bacteria. Thus,
398 expression analysis of genes altered early in the biofilm production process does not support that
399 HBD2 interference with biofilm production occurs at the transcriptional level.
400

401 **Pyorubin accumulation is not reduced in media collected from HBD2 treated *P. aeruginosa***

402 Pigment production in *P. aeruginosa* has been shown to be also regulated by QS [24; 61]. To further
403 corroborate that HBD2 does not interfere with QS, we quantified pyorubin released into culture
404 supernatants in the presence and absence of HBD2. At 0.125 and 0.25 μ M HBD2 there was no
405 difference in pyorubin accumulation compared to the control (data not shown). In the presence of 0.5
406 and 1 μ M HBD2, there was a slight increase of pyorubin ($109.5 \pm 4.9\%$ and $109.9 \pm 5.8\%$ of the
407 control, respectively, $p < 0.01$ in univariate ANOVA with Bonferroni posthoc adjustment). This
408 finding further supports that HBD2 does not inhibit quorum sensing and next, we explored whether
409 HBD2 may induce structural changes in the outer membrane that could interfere with the transport of
410 biofilm precursors to the extracellular space.
411
412

413 **HBD2 alters the outer membrane protein profile of *P. aeruginosa***

414 Outer membrane proteins participate in the process of biofilm formation [78]. Hence, we probed
415 whether incubation with HBD2 leads to changes in the outer membrane protein profile of *P.*
416 *aeruginosa* (Figure 8). A representative image of outer membrane preparations resolved by silver
417 stained SDS-PAGE is depicted in Figure 8A. Numerous bands are detected ranging from about 10
418 kDa to over 200 kDa with the most dominant bands appearing above 25 kDa, in particular a band
419 around 35 kDa similar to the molecular weights of previously reported *P. aeruginosa* outer

420 membrane proteins [79]. Two weaker bands around 10 kDa are consistently visible only in the outer
421 membrane preparations from control bacteria. Overall, the outer membranes from HBD2 treated
422 bacteria appear to contain less proteins between 35 and 75kDa. A prominent band between 10 and 15
423 kDa is detected in all samples, including the medium control, consistent with the molecular weight of
424 the lysozyme (14 kDa) added during the extraction procedure. **Figure 8B** summarizes the protein
425 profiles of the outer membrane preparations from control bacteria and HBD2 treated bacteria. To
426 control for variations during the ultrafiltration process and gel loading, the band intensities of the
427 various proteins were normalized with the presumptive lysozyme band intensity. HBD2 appears to
428 affect a decrease in outer membrane proteins in particular at about 22 kDa, 34 kDa, 40 kDa, 45 kDa,
429 and 50 kDa, with the changes noticeable at all concentrations tested.

430

431

432

433 **Atomic force microscopy reveals ultrastructural changes in HBD2 treated bacteria reflected in 434 increased surface roughness**

435 We also assessed whether the changes at the outer membrane induced by HBD2 resulted in
436 topographical changes and employed atomic force microscopy to measure bacterial height and
437 roughness after incubation for 18 h in the presence or absence of 0.25 μ M HBD2 (**Figure 9**).
438 Representative images of control and HBD2 treated bacteria are shown in **Figure 9A**. The surface of
439 control bacteria appears smoother compared to the surface of HBD2 treated bacteria, the latter
440 showing irregular dents. While the overall bacterial height is not significantly different in HBD2-
441 treated bacteria compared to solvent only exposed bacteria (215.22 ± 3.96 nm *versus* 220.24 ± 3.23
442 nm, means \pm S.E.M, n = 85 and n = 69, respectively, $p = 0.343$), there is a significant increase in
443 roughness in HBD2 treated samples (**Figure 9B**) consistent with a structurally altered surface (43.39 ± 1.52
444 *versus* 51.86 ± 1.5 nm, means \pm S.E.M., n = 85 and n = 69, $p < 0.001$ in independent samples
445 T test).

446

447

448 Taken together, our data demonstrate that at low concentrations L- and D-forms of HBD2 inhibit
449 biofilm formation while not reducing metabolic activity in Gram-negative bacteria of two different
450 genera, *Pseudomonas* and *Acinetobacter*. Furthermore, this activity appears to be receptor-
451 independent and not mediated by interference with quorum sensing or other regulatory pathways of
452 biofilm production at the transcriptional level. Instead, our data are consistent with structural changes
453 induced by HBD2 that interfere with the transport of biofilm precursors into the extracellular space
454 suggesting a novel mechanism of action for the antimicrobial peptide HBD2.

455

456

457 **Discussion**

458

459 In this study, we demonstrate that, HBD2, at nanomolar concentrations, and independent of its chiral
460 state, significantly reduced biofilm formation of *P. aeruginosa* without affecting metabolic activity.
461 This was unlike HBD3, which equally reduced biofilm and metabolic activity at nanomolar
462 concentrations. HBD2 similarly affected *A. baumannii*, another Gram-negative bacterium, at low
463 concentrations. *In silico* modeling did not support direct binding of HBD2 to QS molecules, the
464 release of a QS regulated pigment was not inhibited, and the expression of biofilm-related genes was
465 not influenced by HBD2. However, the outer membrane protein profile was altered in HBD2 treated
466 bacteria with reduced representation of several proteins, which was accompanied by increased
467 roughness of the bacterial surface. Taken together, these data support a novel mechanism of biofilm
468 inhibition by HBD2 at low concentrations that is independent of biofilm regulatory pathways but

469 involves structural changes induced by HBD2 that may interfere with the transport of biofilm
470 precursors into the extracellular space.

471
472 HBD2 has been previously reported to reduce bacterial survival in existing biofilm cultures of
473 *Lactobacillus* ssp., Gram-positive bacteria, at higher, micromolar concentrations. [80]. However,
474 inhibition of biofilm formation by HBD2 has not been reported previously to the best of our
475 knowledge. Considering the rapid induction of HBD2 in epithelial cells' response to
476 proinflammatory cytokines and bacterial challenge [81], the ability to interfere with biofilm
477 formation at low concentrations adds importance to the role of HBD2 in innate host defense during
478 the early interaction between host and pathogen. Bacteria are more susceptible to host-derived and
479 exogenous antimicrobial agents while they are metabolically active in the planktonic state prior to
480 biofilm production. Thus, HBD2 may amplify host defenses early in the attempted infection process
481 and could improve the action of antibiotics in a clinical setting [82]. Synergism studies will be able to
482 address this experimentally in the future.

483
484 Anti-biofilm activity of HBD2 in the absence of inhibition of metabolic activity of *P. aeruginosa*
485 occurred only at low concentrations. A concentration dependent mechanism of action has been well
486 documented for the lantibiotic nisin, which, at nanomolar concentrations, preferentially binds to lipid
487 II disrupting cell wall synthesis and, at micromolar concentrations, embeds into the bacterial
488 membrane causing pore formation [83; 84; 85; 86; 87]. More recently, the alpha-defensin human
489 neutrophil peptide 1 (HNP1) has been added to the list of antimicrobial peptides that initially interact
490 with lipid II, and when concentrations increase, with the bacterial cell membrane [88]. Binding of
491 HBD3 to lipid II has also been described, albeit at higher concentrations, in the micromolar range
492 [47]. It is conceivable that HBD2 could similarly interfere with membrane-embedded proteins
493 responsible for the transport of biofilm components [17] at low concentrations followed by
494 membrane perturbation at higher concentrations.

495
496 The differential effect of HBD2 on biofilm production and metabolic activity of *P. aeruginosa* was
497 not observed in the related beta-defensin HBD3, which was active at lower concentrations than
498 HBD2 and equally reduced biofilm and metabolic activity reflecting a strong bactericidal activity.
499 These differences in their activity could be at least in part attributed to the differences in their
500 physicochemical properties with respect to net charge, surface charge distribution, hydrophobicity
501 index, and behaviour in solution [51; 89]. Biofilm is a complex matrix with numerous components
502 that can be affected in different ways by HBD2 and HBD3. For example, alginate has been shown to
503 affect antimicrobial peptide conformation inducing alpha-helices contingent on the hydrophobicity
504 [90], and HBD2 and HBD3 substantially differ in their hydrophobicity with HBD2 being more
505 hydrophobic than HBD3.

506
507 HBD2, at low concentrations, similarly inhibited biofilm production in *A. baumannii* without
508 reducing metabolic activity suggesting the observed effects are not strain specific. However, at higher
509 HBD2 concentrations differences between the effects on *P. aeruginosa* and *A. baumannii* emerged as
510 reflected in a near complete inhibition of biofilm production of *A. baumannii* contrasting the stalled
511 biofilm inhibition of *P. aeruginosa*. The lesser susceptibility of *P. aeruginosa* to HBD2 may be due
512 to a greater outer membrane vesicle production in *P. aeruginosa* that may sequester HBD2 before it
513 reaches the bacterial cell [91].

514
515 Like other defensins, HBD2 forms three intramolecular disulfide bridges and linearization of the
516 peptide can reveal the importance of its structure for its antimicrobial activity [92]. Here,
517 linearization of full length HBD2 led to a pronounced loss of both its antimicrobial and biofilm

518 inhibitory activity. This contrasts reports for other defensins including HBD3 and could be attributed
519 to a lack of accumulation of positively charged amino acid residues at the C-terminus of HBD2
520 compared to HBD3. Chandrababu and colleagues [93] have shown that positively charged residues
521 cluster in the C-terminal segment of a linearized form of HBD3 allowing them to interact with the
522 negatively charged phospholipids of micelles. The inherent antimicrobial activity of this patch of
523 cationic residues is also reflected in studies with HBD3 analogues truncated to the C-terminal region
524 [94]. The here observed loss of activity after linearization could indicate that HBD2 functions
525 through a receptor [56]. However, D- and L forms of HBD2 did not differ in their activity and thus,
526 we interrogated the possibility that HBD2 interferes with regulatory networks of biofilm production.
527

528 QS molecules are key to the regulation of virulence factor production including biofilm and pigment
529 in *P. aeruginosa*. They are small hydrophobic molecules [95] and thus, we interrogated possible
530 binding of HBD2 to QS molecules *in silico*. We found favorable binding of LasR to not only its
531 cognate ligand 3-oxo-C12-HSL but also to C4-HSL and PQS. This is in line with a recent study
532 describing LasR as promiscuous for binding a variety of QS molecules [96]. The unfavorable binding
533 energies derived for HBD2 suggest that interference of QS-dependent processes through direct
534 HBD2 binding to individual QS molecules is unlikely. Another type of QS molecule, (2S,4S)-2-
535 methyl-2,3,3,4-tetrahydroxytetrahydrofuran-borate (S-THMF-borate), has been shown to increase
536 biofilm formation in *P. aeruginosa* [97; 98]. However, although S-THMF-borate – a molecule with a
537 distinct structure from major Gram-negative QS molecules – has been identified in some Gram-
538 positive and Gram-negative bacteria [99], *P. aeruginosa* does not encode the *luxS* gene required for
539 its synthesis [100] and binding to this S-THMF-borate should not be further considered as an
540 underlying mechanism for the observed biofilm inhibition.
541

542 In agreement with the *in silico* data, HBD2 did not affect the expression of *flgF* and *pslA*. Thus,
543 interference of HBD2 with regulatory networks at the transcriptional level is not likely to account for
544 its biofilm inhibitory activity. However, we cannot rule out that HBD2 has posttranscriptional effects
545 through interference with the two component signal transduction system GacS/GacA [71; 101]. GacS
546 is a transmembrane sensor kinase phosphorylating GacA, which in turn induces the expression of
547 small RNA molecules that antagonize the protein RsmA, a translational repressor interfering with *psl*
548 translation and known to normally block exopolysaccharide production[102]. It is conceivable that
549 HBD2 could interfere with GacS upon inserting into the bacterial membrane. Finally, HBD2 might
550 bind to the secondary messenger molecule c-di-GMP, which regulates biofilm formation in *P.*
551 *aeruginosa* at multiple levels [103]. Previously, de la Fuente-Nunez and colleagues [104]
552 demonstrated that peptide 1018, derived from the antimicrobial peptide bovine Bac2a [105], inhibited
553 biofilm formation in *P. aeruginosa* while not affecting planktonic growth by binding to the second
554 messenger p(pp)Gpp and promoting its degradation. A similar mode of action could apply to HBD2.
555

556 Further supporting that HBD2 does not act through interference with regulatory networks is our
557 finding that pyorubin accumulation in the extracellular fluid was not diminished after incubation with
558 HBD2. Pyorubin is composed of several pigments including aeruginosin A, which is a phenazine,
559 like the much better studied *P. aeruginosa* pigment pyocyanin [106]. Phenazines typically traverse
560 the bacterial membrane freely and their production is under the same controls that govern biofilm
561 production [107; 108].
562

563 Considering the lack of evidence for interference with regulatory networks and the stereoisometry
564 independent activity of HBD2, we conceived that the observed HBD2 mediated inhibition of biofilm
565 production is most likely due to embedding in the bacterial membrane and disruption of transport of
566 biofilm precursor molecules across the membrane. An increasing amount of research suggests that

567 antimicrobial peptides can target discrete loci in bacterial membranes and thereby disrupt biological
568 processes [109]. For example, antimicrobial peptides are known to impair the assembly of
569 multicomponent enzyme complexes in the bacterial cell membrane [110] or disrupt periplasmic
570 protein-protein interaction interfering with molecular transport [111]. In 2013, Kandaswamy and
571 colleagues showed that HBD2 localizes to the mid-cell region of the Gram-positive bacterium *E.*
572 *faecalis* [112]. The authors determined that this mid-cell region is rich in anionic phospholipids and
573 that HBD2 delocalized the spatial organization of protein translocase SecA and sortases, both of
574 which are important for pilus biogenesis [112; 113]. It is possible that HBD2 targets similar
575 machinery in *P. aeruginosa* to impair biofilm formation. SecA also plays a role in the transport of
576 outer membrane proteins in Gram-negative bacteria [114] and outer membrane proteins have been
577 shown to participate in biofilm formation, including the 11 kDa LecB protein and the 38 kDa OprF
578 [115; 116]. Consistent with this we found an altered outer membrane protein profile in HBD2 treated
579 bacteria with a paucity of proteins around 10kDa and proteins around the molecular weights of
580 previously reported outer membrane proteins. This may indicate structural changes of the outer
581 membrane, which was further supported by our atomic force microscopy data demonstrating an
582 increased roughness of the bacterial surface after HBD2 treatment. It is important to note, however,
583 that increased roughness could also represent changes in the LPS profile. Atomic force microscopy
584 has been previously employed elsewhere to demonstrate outer membrane damages in *P. aeruginosa*
585 [117]. Resolving the outer membrane proteins by 2D gel electrophoresis could further delineate the
586 observed changes in future experiments, which should also revisit the action of the D form of HBD2
587 and effects on the outer membrane of *A. baumannii*. Finally, outer membrane vesicles have been
588 recognized to take part in the formation of biofilm by interacting with extracellular DNA and HBD2
589 interference with proper outer membrane formation may disrupt this process [118].
590

591 In conclusion, this study reveals distinct activity of two epithelial beta-defensins, HBD2 and HBD3,
592 and provides evidence for a novel antibacterial action of HBD2. At low concentrations in the
593 nanomolar range, HBD2 reduced biofilm formation without reducing the metabolic activity of *P.*
594 *aeruginosa*. Biofilm production of *A. baumannii* was similarly affected, indicating that the observed
595 HBD2 activity is not strain specific. This activity is unlikely mediated through a receptor-dependent
596 interference with regulatory networks but contingent on preservation of HBD2 structure. Our
597 findings are consistent with a membrane-targeted action of HBD2 that affects proper function of
598 membrane-associated proteins involved in biofilm precursor transport into the extracellular
599 environment. Future studies dissecting the molecular basis for the described HBD2 activity may
600 inform the development of new methods for the manipulation of biofilms in aquaculture, in the food
601 industry, and in the healthcare setting, which is in particular of interest for the latter considering the
602 rise of multidrug resistance.
603

604 **Conflict of Interest**

605 The authors declare that the research was conducted in the absence of any commercial or financial
606 relationships that could be construed as a potential conflict of interest.
607

608 **Author Contributions**

609 KRP, BB, TY, MB, EE, ATT, AC, and YW: acquisition of data. KRP, BB, TY, MB, EE, ATT, AC,
610 HP, YW, WL, and EP: analysis and interpretation of data. KRP, MM, and CA: method development.
611 KRP and EP: statistical analysis. KRP: molecular docking. KRP, HP, YW, WL, and EP: conceptual
612 and experimental design. KRP, HP, and EP: drafted manuscript. KRP, BB, TY, MB, EE, ATT, AC,
613 MM, CA, HP, YW, WL, and EP: critical revision of the manuscript for important intellectual
614 content. All authors approved the final manuscript submission.
615

616 **Funding**

617 The authors disclosed receipt of the following financial support for the research, authorship, and/or
618 publication of this article: This work was supported by the National Institutes of Health [grants NIH
619 SC1 GM096916, NIH RISE GM061331 and NIH LA Basin Bridges to PhD GM054939], the
620 National Science Foundation [grant NSF-MRI 1828334], the California State University Library
621 Open Access Author Fund, and the College of Natural and Social Sciences at California State
622 University Los Angeles [NSS Research and Scholarship Award 2018]. The funders provided no input
623 to the study design nor in the collection, analyses and interpretation of data.

624

625 **Acknowledgments**

626 We thank Susan Cohen for helpful discussions. Parts of the result presented here have been included
627 in the Master's Thesis of KRP [119] and presented at the Microbe 2019 General Meeting of the
628 American Society for Microbiology in San Francisco, CA, June 20 – 24, 2019.

629

630

631 **Contribution to the Field**

632 Biofilms are microbial communities enwrapped in a sticky substance made out of carbohydrates,
633 proteins, and extracellular DNA. They are formed in water environments but also on body surfaces
634 where they often precede the development of infectious disease and protect the microbes against host
635 immune factors and antibiotics. The bacterium *P. aeruginosa* is known to produce biofilms in
636 patients with a compromised immune system contributing to significant health care burden that is
637 aggravated by the increasing resistance to antibiotics. Novel approaches to prevent and treat biofilm-
638 associated infections are needed and innate immune factors that normally prevent infections with *P.*
639 *aeruginosa* may inform new drug design. Antimicrobial peptides are ancient natural antimicrobial
640 substances that are widely conserved in nature, underlining their importance for homeostasis. Yet,
641 different organisms express their own repertoires and antimicrobial peptide expression varies within
642 an organism pointing to unique localized functions. In this study, we unveil a novel, distinct action of
643 the epithelial antimicrobial peptide human beta-defensin 2 adding to its known mechanisms of action
644 and providing a better understanding why immunocompetent individuals are protected against *P.*
645 *aeruginosa* colonization and infections. This research may lead to the identification of novel targets
646 for the engineering of antimicrobials.

647

648 **Data Availability Statement**

649 Datasets are available on request. The raw data supporting the conclusions of this manuscript will be
650 made available by the authors, without undue reservation, to any qualified researcher.

651

652

653 **References**

- 654 [1] P.Y. Qian, S.C. Lau, H.U. Dahms, S. Dobretsov, and T. Harder, Marine biofilms as mediators of
655 colonization by marine macroorganisms: implications for antifouling and aquaculture. *Marine
656 biotechnology* (New York, N.Y.) 9 (2007) 399-410.
- 657 [2] P.K. Taylor, A.T. Yeung, and R.E. Hancock, Antibiotic resistance in *Pseudomonas aeruginosa*
658 biofilms: towards the development of novel anti-biofilm therapies. *Journal of biotechnology*
659 191 (2014) 121-30.
- 660 [3] M. Wilton, L. Charron-Mazenod, R. Moore, and S. Lewenza, Extracellular DNA Acidifies
661 Biofilms and Induces Aminoglycoside Resistance in *Pseudomonas aeruginosa*. *Antimicrobial
662 agents and chemotherapy* 60 (2016) 544-53.

663 [4] R.M. Donlan, and J.W. Costerton, Biofilms: survival mechanisms of clinically relevant
664 microorganisms. *Clin Microbiol Rev* 15 (2002) 167-93.

665 [5] N. Hoiby, T. Bjarnsholt, M. Givskov, S. Molin, and O. Ciofu, Antibiotic resistance of bacterial
666 biofilms. *International journal of antimicrobial agents* 35 (2010) 322-32.

667 [6] L.K. Jennings, K.M. Storek, H.E. Ledvina, C. Coulon, L.S. Marmont, I. Sadovskaya, P.R. Secor,
668 B.S. Tseng, M. Scian, A. Filloux, D.J. Wozniak, P.L. Howell, and M.R. Parsek, Pel is a
669 cationic exopolysaccharide that cross-links extracellular DNA in the *Pseudomonas aeruginosa*
670 biofilm matrix. *Proceedings of the National Academy of Sciences of the United States of*
671 *America* 112 (2015) 11353-8.

672 [7] K.M. Colvin, Y. Irie, C.S. Tart, R. Urbano, J.C. Whitney, C. Ryder, P.L. Howell, D.J. Wozniak,
673 and M.R. Parsek, The Pel and Psl polysaccharides provide *Pseudomonas aeruginosa* structural
674 redundancy within the biofilm matrix. *Environmental microbiology* 14 (2012) 1913-28.

675 [8] T.B. May, D. Shinabarger, R. Maharaj, J. Kato, L. Chu, J.D. DeVault, S. Roychoudhury, N.A.
676 Zielinski, A. Berry, R.K. Rothmel, and et al., Alginic synthesis by *Pseudomonas aeruginosa*:
677 a key pathogenic factor in chronic pulmonary infections of cystic fibrosis patients. *Clin*
678 *Microbiol Rev* 4 (1991) 191-206.

679 [9] J.N.C. Fong, and F.H. Yildiz, Biofilm Matrix Proteins. *Microbiology spectrum* 3 (2015).

680 [10] L. Turnbull, M. Toyofuku, A.L. Hynen, M. Kurosawa, G. Pessi, N.K. Petty, S.R. Osvath, G.
681 Carcamo-Oyarce, E.S. Gloag, R. Shimoni, U. Omasits, S. Ito, X. Yap, L.G. Monahan, R.
682 Cavaliere, C.H. Ahrens, I.G. Charles, N. Nomura, L. Eberl, and C.B. Whitchurch, Explosive
683 cell lysis as a mechanism for the biogenesis of bacterial membrane vesicles and biofilms.
684 *Nature communications* 7 (2016) 11220.

685 [11] C.B. Whitchurch, T. Tolker-Nielsen, P.C. Ragas, and J.S. Mattick, Extracellular DNA required
686 for bacterial biofilm formation. *Science (New York, N.Y.)* 295 (2002) 1487.

687 [12] T. Das, S. Sehar, and M. Manefield, The roles of extracellular DNA in the structural integrity of
688 extracellular polymeric substance and bacterial biofilm development. *Environmental*
689 *microbiology reports* 5 (2013) 778-86.

690 [13] O.E. Petrova, and K. Sauer, Sticky situations: key components that control bacterial surface
691 attachment. *Journal of bacteriology* 194 (2012) 2413-25.

692 [14] B. Stojkovic, S. Sretenovic, I. Dogsa, I. Poberaj, and D. Stopar, Viscoelastic properties of levan-
693 DNA mixtures important in microbial biofilm formation as determined by micro- and
694 macrorheology. *Biophysical journal* 108 (2015) 758-65.

695 [15] K.N. Cowles, and Z. Gitai, Surface association and the MreB cytoskeleton regulate pilus
696 production, localization and function in *Pseudomonas aeruginosa*. *Molecular microbiology* 76
697 (2010) 1411-26.

698 [16] J.P. Pearson, L. Passador, B.H. Iglewski, and E.P. Greenberg, A second N-acylhomoserine
699 lactone signal produced by *Pseudomonas aeruginosa*. *Proceedings of the National Academy*
700 *of Sciences of the United States of America* 92 (1995) 1490-4.

701 [17] G. Laverty, S.P. Gorman, and B.F. Gilmore, Biomolecular Mechanisms of *Pseudomonas*
702 *aeruginosa* and *Escherichia coli* Biofilm Formation. *Pathogens* 3 (2014) 596-632.

703 [18] S.T. Rutherford, and B.L. Bassler, Bacterial quorum sensing: its role in virulence and
704 possibilities for its control. *Cold Spring Harbor perspectives in medicine* 2 (2012).

705 [19] J. Overhage, M. Schemionek, J.S. Webb, and B.H. Rehm, Expression of the psl operon in
706 *Pseudomonas aeruginosa* PAO1 biofilms: PslA performs an essential function in biofilm
707 formation. *Applied and environmental microbiology* 71 (2005) 4407-13.

708 [20] Y. Irie, M. Starkey, A.N. Edwards, D.J. Wozniak, T. Romeo, and M.R. Parsek, *Pseudomonas*
709 *aeruginosa* biofilm matrix polysaccharide Psl is regulated transcriptionally by RpoS and post-
710 transcriptionally by RsmA. *Molecular microbiology* 78 (2010) 158-72.

711 [21] A.R. Hauser, The type III secretion system of *Pseudomonas aeruginosa*: infection by injection.
712 *Nature reviews. Microbiology* 7 (2009) 654-65.

713 [22] L. Zulianello, C. Canard, T. Kohler, D. Caille, J.S. Lacroix, and P. Meda, Rhamnolipids are
714 virulence factors that promote early infiltration of primary human airway epithelia by
715 *Pseudomonas aeruginosa*. *Infection and immunity* 74 (2006) 3134-47.

716 [23] Z. Hosseiniidoust, N. Tufenkji, and T.G. van de Ven, Predation in homogeneous and
717 heterogeneous phage environments affects virulence determinants of *Pseudomonas*
718 *aeruginosa*. *Applied and environmental microbiology* 79 (2013) 2862-71.

719 [24] V. Naik, and G. Mahajan, Quorum sensing: a non-conventional target for antibiotic discovery.
720 *Natural product communications* 8 (2013) 1455-8.

721 [25] V.T. Orlandi, F. Bolognese, L. Chiodaroli, T. Tolker-Nielsen, and P. Barbieri, Pigments
722 influence the tolerance of *Pseudomonas aeruginosa* PAO1 to photodynamically induced
723 oxidative stress. *Microbiology* 161 (2015) 2298-309.

724 [26] J.A. Driscoll, S.L. Brody, and M.H. Kollef, The epidemiology, pathogenesis and treatment of
725 *Pseudomonas aeruginosa* infections. *Drugs* 67 (2007) 351-68.

726 [27] M. Zasloff, Antibiotic peptides as mediators of innate immunity. *Current opinion in*
727 *immunology* 4 (1992) 3-7.

728 [28] C.L. Bevins, Antimicrobial peptides as effector molecules of mammalian host defense.
729 *Contributions to microbiology* 10 (2003) 106-48.

730 [29] E. Martin, T. Ganz, and R.I. Lehrer, Defensins and other endogenous peptide antibiotics of
731 vertebrates. *Journal of leukocyte biology* 58 (1995) 128-36.

732 [30] A. Oren, T. Ganz, L. Liu, and T. Meerloo, In human epidermis, beta-defensin 2 is packaged in
733 lamellar bodies. *Experimental and molecular pathology* 74 (2003) 180-2.

734 [31] L. Liu, L. Wang, H.P. Jia, C. Zhao, H.H. Heng, B.C. Schutte, P.B. McCray, Jr., and T. Ganz,
735 Structure and mapping of the human beta-defensin HBD-2 gene and its expression at sites of
736 inflammation. *Gene* 222 (1998) 237-44.

737 [32] C.J. Hertz, Q. Wu, E.M. Porter, Y.J. Zhang, K.H. Weismuller, P.J. Godowski, T. Ganz, S.H.
738 Randell, and R.L. Modlin, Activation of Toll-like receptor 2 on human tracheobronchial
739 epithelial cells induces the antimicrobial peptide human beta defensin-2. *Journal of*
740 *immunology* (Baltimore, Md. : 1950) 171 (2003) 6820-6.

741 [33] G. Wang, Human antimicrobial peptides and proteins. *Pharmaceuticals* (Basel, Switzerland) 7
742 (2014) 545-94.

743 [34] K. Matsuzaki, Membrane Permeabilization Mechanisms. *Advances in experimental medicine*
744 and biology 1117 (2019) 9-16.

745 [35] J.C. Bozelli, Jr., E.T. Sasahara, M.R. Pinto, C.R. Nakaie, and S. Schreier, Effect of head group
746 and curvature on binding of the antimicrobial peptide tritrypticin to lipid membranes.
747 Chemistry and physics of lipids 165 (2012) 365-73.

748 [36] E. Strandberg, D. Tiltak, S. Ehni, P. Wadhwan, and A.S. Ulrich, Lipid shape is a key factor for
749 membrane interactions of amphipathic helical peptides. Biochimica et biophysica acta 1818
750 (2012) 1764-76.

751 [37] E. Strandberg, J. Zerweck, P. Wadhwan, and A.S. Ulrich, Synergistic insertion of antimicrobial
752 magainin-family peptides in membranes depends on the lipid spontaneous curvature.
753 Biophysical journal 104 (2013) L9-11.

754 [38] S. Afonin, R.W. Glaser, C. Sachse, J. Salgado, P. Wadhwan, and A.S. Ulrich, (19)F NMR
755 screening of unrelated antimicrobial peptides shows that membrane interactions are largely
756 governed by lipids. Biochimica et biophysica acta 1838 (2014) 2260-8.

757 [39] B.S. Perrin, Jr., A.J. Sodt, M.L. Cotten, and R.W. Pastor, The Curvature Induction of Surface-
758 Bound Antimicrobial Peptides Piscidin 1 and Piscidin 3 Varies with Lipid Chain Length. The
759 Journal of membrane biology 248 (2015) 455-67.

760 [40] D.J. Paterson, M. Tassieri, J. Reboud, R. Wilson, and J.M. Cooper, Lipid topology and
761 electrostatic interactions underpin lytic activity of linear cationic antimicrobial peptides in
762 membranes. Proceedings of the National Academy of Sciences of the United States of
763 America 114 (2017) E8324-e8332.

764 [41] K.A. Brogden, Antimicrobial peptides: pore formers or metabolic inhibitors in bacteria? Nature
765 reviews. Microbiology 3 (2005) 238-50.

766 [42] A. Fabisiak, N. Murawska, and J. Fichna, LL-37: Cathelicidin-related antimicrobial peptide with
767 pleiotropic activity. Pharmacological reports : PR 68 (2016) 802-8.

768 [43] J. Overhage, A. Campisano, M. Bains, E.C. Torfs, B.H. Rehm, and R.E. Hancock, Human host
769 defense peptide LL-37 prevents bacterial biofilm formation. Infection and immunity 76
770 (2008) 4176-82.

771 [44] C. Nagant, B. Pitts, K. Nazmi, M. Vandenbranden, J.G. Bolscher, P.S. Stewart, and J.P. Dehaye,
772 Identification of peptides derived from the human antimicrobial peptide LL-37 active against
773 biofilms formed by *Pseudomonas aeruginosa* using a library of truncated fragments.
774 Antimicrobial agents and chemotherapy 56 (2012) 5698-708.

775 [45] C. Koro, A. Hellvard, N. Delaleu, V. Binder, C. Scavenius, B. Bergum, I. Glowczyk, H.M.
776 Roberts, I.L. Chapple, M.M. Grant, M. Rapala-Kozik, K. Klaga, J.J. Enghild, J. Potempa, and
777 P. Mydel, Carbamylated LL-37 as a modulator of the immune response. Innate immunity 22
778 (2016) 218-29.

779 [46] Y. Kai-Larsen, and B. Agerberth, The role of the multifunctional peptide LL-37 in host defense.
780 Frontiers in bioscience : a journal and virtual library 13 (2008) 3760-7.

781 [47] V. Sass, T. Schneider, M. Wilmes, C. Korner, A. Tossi, N. Novikova, O. Shamova, and H.G.
782 Sahl, Human beta-defensin 3 inhibits cell wall biosynthesis in *Staphylococci*. Infection and
783 immunity 78 (2010) 2793-800.

784 [48] N. Kanda, M. Kamata, Y. Tada, T. Ishikawa, S. Sato, and S. Watanabe, Human beta-defensin-2
785 enhances IFN-gamma and IL-10 production and suppresses IL-17 production in T cells.
786 Journal of leukocyte biology 89 (2011) 935-44.

787 [49] A.B. Estrela, M. Rohde, M.G. Gutierrez, G. Molinari, and W.R. Abraham, Human beta-defensin
788 2 induces extracellular accumulation of adenosine in Escherichia coli. *Antimicrobial agents*
789 and chemotherapy 57 (2013) 4387-93.

790 [50] D. Yang, O. Chertov, S.N. Bykovskaia, Q. Chen, M.J. Buffo, J. Shogan, M. Anderson, J.M.
791 Schroder, J.M. Wang, O.M. Howard, and J.J. Oppenheim, Beta-defensins: linking innate and
792 adaptive immunity through dendritic and T cell CCR6. *Science (New York, N.Y.)* 286 (1999)
793 525-8.

794 [51] B. Spudy, F.D. Sonnichsen, G.H. Waetzig, J. Grotzinger, and S. Jung, Identification of structural
795 traits that increase the antimicrobial activity of a chimeric peptide of human beta-defensins 2
796 and 3. *Biochemical and biophysical research communications* 427 (2012) 207-11.

797 [52] D.M. Hoover, Z. Wu, K. Tucker, W. Lu, and J. Lubkowski, Antimicrobial characterization of
798 human beta-defensin 3 derivatives. *Antimicrobial agents and chemotherapy* 47 (2003) 2804-
799 9.

800 [53] V. Dhople, A. Krukemeyer, and A. Ramamoorthy, The human beta-defensin-3, an antibacterial
801 peptide with multiple biological functions. *Biochimica et biophysica acta* 1758 (2006) 1499-
802 512.

803 [54] O.N. Silva, W.F. Porto, S.M. Ribeiro, I. Batista, and O.L. Franco, Host-defense peptides and
804 their potential use as biomarkers in human diseases. *Drug discovery today* 23 (2018) 1666-
805 1671.

806 [55] E. Galdiero, L. Lombardi, A. Falanga, G. Libralato, M. Guida, and R. Carotenuto, *Biofilms: Novel Strategies Based on Antimicrobial Peptides*. *Pharmaceutics* 11 (2019).

807 [56] Z. Wu, D.M. Hoover, D. Yang, C. Boulegue, F. Santamaria, J.J. Oppenheim, J. Lubkowski, and
808 W. Lu, Engineering disulfide bridges to dissect antimicrobial and chemotactic activities of
809 human beta-defensin 3. *Proceedings of the National Academy of Sciences of the United
810 States of America* 100 (2003) 8880-5.

811 [57] G. Wei, E. de Leeuw, M. Pazgier, W. Yuan, G. Zou, J. Wang, B. Ericksen, W.Y. Lu, R.I.
812 Lehrer, and W. Lu, Through the looking glass, mechanistic insights from enantiomeric human
813 defensins. *The Journal of biological chemistry* 284 (2009) 29180-92.

814 [58] J.H. Merritt, D.E. Kadouri, and G.A. O'Toole, Growing and analyzing static biofilms. *Current
815 protocols in microbiology Chapter 1* (2005) Unit 1B.1.

816 [59] M.U. Shiloh, J. Ruan, and C. Nathan, Evaluation of bacterial survival and phagocyte function
817 with a fluorescence-based microplate assay. *Infection and immunity* 65 (1997) 3193-8.

818 [60] J.G. Martinez, M. Waldon, Q. Huang, S. Alvarez, A. Oren, N. Sandoval, M. Du, F. Zhou, A.
819 Zenz, K. Lohner, R. Desharnais, and E. Porter, Membrane-targeted synergistic activity of
820 docosahexaenoic acid and lysozyme against *Pseudomonas aeruginosa*. *The Biochemical
821 journal* 419 (2009) 193-200.

822 [61] E.A. Abu, S. Su, L. Sallans, R.E. Boissy, A. Greatens, W.R. Heineman, and D.J. Hassett, Cyclic
823 voltammetric, fluorescence and biological analysis of purified aeruginosin A, a secreted red
824 pigment of *Pseudomonas aeruginosa* PAO1. *Microbiology* 159 (2013) 1736-47.

825 [62] S. Shityakov, and C. Forster, In silico predictive model to determine vector-mediated transport
826 properties for the blood-brain barrier choline transporter. *Advances and applications in
827 bioinformatics and chemistry : AABC* 7 (2014) 23-36.

829 [63] M. Park, G. Yoo, J.H. Bong, J. Jose, M.J. Kang, and J.C. Pyun, Isolation and characterization of
830 the outer membrane of *Escherichia coli* with autodisplayed Z-domains. *Biochimica et*
831 *biophysica acta* 1848 (2015) 842-7.

832 [64] Y. Chao, and T. Zhang, Optimization of fixation methods for observation of bacterial cell
833 morphology and surface ultrastructures by atomic force microscopy. *Appl Microbiol*
834 *Biotechnol* 92 (2011) 381-92.

835 [65] Y.F. Dufrene, T. Ando, R. Garcia, D. Alsteens, D. Martinez-Martin, A. Engel, C. Gerber, and
836 D.J. Muller, Imaging modes of atomic force microscopy for application in molecular and cell
837 biology. *Nature nanotechnology* 12 (2017) 295-307.

838 [66] J. Rohrl, D. Yang, J.J. Oppenheim, and T. Hehlgans, Human beta-defensin 2 and 3 and their
839 mouse orthologs induce chemotaxis through interaction with CCR2. *Journal of immunology*
840 (Baltimore, Md. : 1950) 184 (2010) 6688-94.

841 [67] J. Rohrl, D. Yang, J.J. Oppenheim, and T. Hehlgans, Specific binding and chemotactic activity
842 of mBD4 and its functional orthologue hBD2 to CCR6-expressing cells. *The Journal of*
843 *biological chemistry* 285 (2010) 7028-34.

844 [68] D.M. Hoover, K.R. Rajashankar, R. Blumenthal, A. Puri, J.J. Oppenheim, O. Chertov, and J.
845 Lubkowski, The structure of human beta-defensin-2 shows evidence of higher order
846 oligomerization. *The Journal of biological chemistry* 275 (2000) 32911-8.

847 [69] M.V. Trivedi, J.S. Laurence, and T.J. Sahaan, The role of thiols and disulfides on protein
848 stability. *Current protein & peptide science* 10 (2009) 614-25.

849 [70] J.N. Onuchic, Z. Luthey-Schulten, and P.G. Wolynes, Theory of protein folding: the energy
850 landscape perspective. *Annual review of physical chemistry* 48 (1997) 545-600.

851 [71] P.N. Jimenez, G. Koch, J.A. Thompson, K.B. Xavier, R.H. Cool, and W.J. Quax, The multiple
852 signaling systems regulating virulence in *Pseudomonas aeruginosa*. *Microbiology and*
853 *molecular biology reviews : MMBR* 76 (2012) 46-65.

854 [72] Y. Zou, and S.K. Nair, Molecular basis for the recognition of structurally distinct autoinducer
855 mimics by the *Pseudomonas aeruginosa* LasR quorum-sensing signaling receptor. *Chemistry*
856 & *biology* 16 (2009) 961-70.

857 [73] C.F. Le, M.Y. Yusof, M.A. Hassan, V.S. Lee, D.M. Isa, and S.D. Sekaran, In vivo efficacy and
858 molecular docking of designed peptide that exhibits potent antipneumococcal activity and
859 synergises in combination with penicillin. *Scientific reports* 5 (2015) 11886.

860 [74] J.D. Moore, F.M. Rossi, M.A. Welsh, K.E. Nyffeler, and H.E. Blackwell, A Comparative
861 Analysis of Synthetic Quorum Sensing Modulators in *Pseudomonas aeruginosa*: New Insights
862 into Mechanism, Active Efflux Susceptibility, Phenotypic Response, and Next-Generation
863 Ligand Design. *Journal of the American Chemical Society* 137 (2015) 14626-39.

864 [75] I.J. Choi, C.S. Rhee, C.H. Lee, and D.Y. Kim, Effect of allergic rhinitis on the expression of
865 human beta-defensin 2 in tonsils. *Annals of allergy, asthma & immunology : official*
866 *publication of the American College of Allergy, Asthma, & Immunology* 110 (2013) 178-83.

867 [76] T. Hiratsuka, M. Nakazato, Y. Date, J. Ashitani, T. Minematsu, N. Chino, and S. Matsukura,
868 Identification of human beta-defensin-2 in respiratory tract and plasma and its increase in
869 bacterial pneumonia. *Biochemical and biophysical research communications* 249 (1998) 943-
870 7.

871 [77] T. Hiratsuka, H. Mukae, H. Iiboshi, J. Ashitani, K. Nabeshima, T. Minematsu, N. Chino, T. Ihi,
872 S. Kohno, and M. Nakazato, Increased concentrations of human beta-defensins in plasma and
873 bronchoalveolar lavage fluid of patients with diffuse panbronchiolitis. *Thorax* 58 (2003) 425-
874 30.

875 [78] S. Chevalier, E. Bouffartigues, J. Bodilis, O. Maillet, O. Lesouhaitier, M.G.J. Feuilloley, N.
876 Orange, A. Dufour, and P. Cornelis, Structure, function and regulation of *Pseudomonas*
877 *aeruginosa* porins. *FEMS microbiology reviews* 41 (2017) 698-722.

878 [79] R.E. Hancock, R. Siehnel, and N. Martin, Outer membrane proteins of *Pseudomonas*. *Molecular*
879 *microbiology* 4 (1990) 1069-75.

880 [80] J.E. Goeke, S. Kist, S. Schubert, R. Hickel, K.C. Huth, and M. Kollmuss, Sensitivity of caries
881 pathogens to antimicrobial peptides related to caries risk. *Clinical oral investigations* 22
882 (2018) 2519-2525.

883 [81] D.A. O'Neil, S.P. Cole, E. Martin-Porter, M.P. Housley, L. Liu, T. Ganz, and M.F. Kagnoff,
884 Regulation of human beta-defensins by gastric epithelial cells in response to infection with
885 *Helicobacter pylori* or stimulation with interleukin-1. *Infection and immunity* 68 (2000) 5412-
886 5.

887 [82] A. Crabbe, L. Ostyn, S. Staelens, C. Rigauts, M. Risseeuw, M. Dhaenens, S. Daled, H. Van
888 Acker, D. Deforce, S. Van Calenbergh, and T. Coenye, Host metabolites stimulate the
889 bacterial proton motive force to enhance the activity of aminoglycoside antibiotics. *PLoS*
890 *pathogens* 15 (2019) e1007697.

891 [83] K.M. Scherer, J.H. Spille, H.G. Sahl, F. Grein, and U. Kubitscheck, The lantibiotic nisin induces
892 lipid II aggregation, causing membrane instability and vesicle budding. *Biophysical journal*
893 108 (2015) 1114-24.

894 [84] C. van Kraaij, E. Breukink, M.A. Noordermeer, R.A. Demel, R.J. Siezen, O.P. Kuipers, and B.
895 de Kruijff, Pore formation by nisin involves translocation of its C-terminal part across the
896 membrane. *Biochemistry* 37 (1998) 16033-40.

897 [85] K. Winkowski, R.D. Ludescher, and T.J. Montville, Physiochemical characterization of the
898 nisin-membrane interaction with liposomes derived from *Listeria monocytogenes*. *Applied*
899 *and environmental microbiology* 62 (1996) 323-7.

900 [86] M.J. Garcera, M.G. Elferink, A.J. Driessen, and W.N. Konings, In vitro pore-forming activity of
901 the lantibiotic nisin. Role of protonmotive force and lipid composition. *European journal of*
902 *biochemistry / FEBS* 212 (1993) 417-22.

903 [87] G. Bierbaum, and H.G. Sahl, Lantibiotics: mode of action, biosynthesis and bioengineering.
904 *Current pharmaceutical biotechnology* 10 (2009) 2-18.

905 [88] E. de Leeuw, C. Li, P. Zeng, C. Li, M. Diepeveen-de Buin, W.Y. Lu, E. Breukink, and W. Lu,
906 Functional interaction of human neutrophil peptide-1 with the cell wall precursor lipid II.
907 *FEBS letters* 584 (2010) 1543-8.

908 [89] D.J. Schibli, H.N. Hunter, V. Aseyev, T.D. Starner, J.M. Wiencek, P.B. McCray, Jr., B.F. Tack,
909 and H.J. Vogel, The solution structures of the human beta-defensins lead to a better
910 understanding of the potent bactericidal activity of HBD3 against *Staphylococcus aureus*. *The*
911 *Journal of biological chemistry* 277 (2002) 8279-89.

912 [90] C. Chan, L.L. Burrows, and C.M. Deber, Helix induction in antimicrobial peptides by alginate in
913 biofilms. *The Journal of biological chemistry* 279 (2004) 38749-54.

914 [91] C. Perez-Cruz, L. Delgado, C. Lopez-Iglesias, and E. Mercade, Outer-inner membrane vesicles
915 naturally secreted by gram-negative pathogenic bacteria. *PLoS one* 10 (2015) e0116896.

916 [92] B. Mathew, and R. Nagaraj, Antimicrobial activity of human alpha-defensin 6 analogs: insights
917 into the physico-chemical reasons behind weak bactericidal activity of HD6 in vitro. *J Pept
918 Sci* 21 (2015) 811-8.

919 [93] K.B. Chandrababu, B. Ho, and D. Yang, Structure, dynamics, and activity of an all-cysteine
920 mutated human beta defensin-3 peptide analogue. *Biochemistry* 48 (2009) 6052-61.

921 [94] V. Krishnakumari, and R. Nagaraj, Interaction of antibacterial peptides spanning the carboxy-
922 terminal region of human beta-defensins 1-3 with phospholipids at the air-water interface and
923 inner membrane of *E. coli*. *Peptides* 29 (2008) 7-14.

924 [95] L. Mashburn-Warren, J. Howe, P. Garidel, W. Richter, F. Steiniger, M. Roessle, K.
925 Brandenburg, and M. Whiteley, Interaction of quorum signals with outer membrane lipids:
926 insights into prokaryotic membrane vesicle formation. *Molecular microbiology* 69 (2008)
927 491-502.

928 [96] A.R. McCready, J.E. Paczkowski, B.R. Henke, and B.L. Bassler, Structural determinants driving
929 homoserine lactone ligand selection in the *Pseudomonas aeruginosa* LasR quorum-sensing
930 receptor. *Proceedings of the National Academy of Sciences of the United States of America*
931 116 (2019) 245-254.

932 [97] T.J. Tavender, N.M. Halliday, K.R. Hardie, and K. Winzer, LuxS-independent formation of AI-
933 2 from ribulose-5-phosphate. *BMC microbiology* 8 (2008) 98.

934 [98] H. Li, X. Li, Z. Wang, Y. Fu, Q. Ai, Y. Dong, and J. Yu, Autoinducer-2 regulates *Pseudomonas*
935 *aeruginosa* PAO1 biofilm formation and virulence production in a dose-dependent manner.
936 *BMC microbiology* 15 (2015) 192.

937 [99] M.B. Miller, and B.L. Bassler, Quorum sensing in bacteria. *Annual review of microbiology* 55
938 (2001) 165-99.

939 [100] K. Duan, C. Dammel, J. Stein, H. Rabin, and M.G. Surette, Modulation of *Pseudomonas*
940 *aeruginosa* gene expression by host microflora through interspecies communication.
941 *Molecular microbiology* 50 (2003) 1477-91.

942 [101] Q. Wei, and L.Z. Ma, Biofilm matrix and its regulation in *Pseudomonas aeruginosa*.
943 *International journal of molecular sciences* 14 (2013) 20983-1005.

944 [102] H. Mikkelsen, M. Sivaneson, and A. Filloux, Key two-component regulatory systems that
945 control biofilm formation in *Pseudomonas aeruginosa*. *Environmental microbiology* 13
946 (2011) 1666-81.

947 [103] D.G. Ha, and G.A. O'Toole, c-di-GMP and its Effects on Biofilm Formation and Dispersion: a
948 *Pseudomonas Aeruginosa* Review. *Microbiology spectrum* 3 (2015) Mb-0003-2014.

949 [104] C. de la Fuente-Nunez, F. Reffuveille, E.F. Haney, S.K. Straus, and R.E. Hancock, Broad-
950 spectrum anti-biofilm peptide that targets a cellular stress response. *PLoS pathogens* 10
951 (2014) e1004152.

952 [105] L. Steinstraesser, T. Hirsch, M. Schulte, M. Kueckelhaus, F. Jacobsen, E.A. Mersch, I.
953 Stricker, N. Afacan, H. Jenssen, R.E. Hancock, and J. Kindrachuk, Innate defense regulator
954 peptide 1018 in wound healing and wound infection. *PLoS one* 7 (2012) e39373.

955 [106] G.S. Byng, D.C. Eustice, and R.A. Jensen, Biosynthesis of phenazine pigments in mutant and
956 wild-type cultures of *Pseudomonas aeruginosa*. *Journal of bacteriology* 138 (1979) 846-52.

957 [107] A. Bala, L. Kumar, S. Chhibber, and K. Harjai, Augmentation of virulence related traits of pqs
958 mutants by *Pseudomonas* quinolone signal through membrane vesicles. *Journal of basic*
959 *microbiology* 55 (2015) 566-78.

960 [108] Y.L. Lo, L. Shen, C.H. Chang, M. Bhuwan, C.H. Chiu, and H.Y. Chang, Regulation of
961 Motility and Phenazine Pigment Production by FliA Is Cyclic-di-GMP Dependent in
962 *Pseudomonas aeruginosa* PAO1. *PloS one* 11 (2016) e0155397.

963 [109] R. Rashid, M. Veleba, and K.A. Kline, Focal Targeting of the Bacterial Envelope by
964 Antimicrobial Peptides. *Frontiers in cell and developmental biology* 4 (2016) 55.

965 [110] M. Wenzel, A.I. Chiriac, A. Otto, D. Zweytk, C. May, C. Schumacher, R. Gust, H.B. Albada,
966 M. Penkova, U. Kramer, R. Erdmann, N. Metzler-Nolte, S.K. Straus, E. Bremer, D. Becher,
967 H. Brotz-Oesterhelt, H.G. Sahl, and J.E. Bandow, Small cationic antimicrobial peptides
968 delocalize peripheral membrane proteins. *Proceedings of the National Academy of Sciences*
969 of the United States of America 111 (2014) E1409-18.

970 [111] S.U. Vetterli, K. Zerbe, M. Muller, M. Urfer, M. Mondal, S.Y. Wang, K. Moehle, O. Zerbe, A.
971 Vitale, G. Pessi, L. Eberl, B. Wollscheid, and J.A. Robinson, Thanatin targets the
972 intermembrane protein complex required for lipopolysaccharide transport in *Escherichia coli*.
973 *Science advances* 4 (2018) eaau2634.

974 [112] K. Kandaswamy, T.H. Liew, C.Y. Wang, E. Huston-Warren, U. Meyer-Hoffert, K. Hultenby,
975 J.M. Schroder, M.G. Caparon, S. Normark, B. Henriques-Normark, S.J. Hultgren, and K.A.
976 Kline, Focal targeting by human beta-defensin 2 disrupts localized virulence factor assembly
977 sites in *Enterococcus faecalis*. *Proceedings of the National Academy of Sciences of the*
978 *United States of America* 110 (2013) 20230-5.

979 [113] H.V. Nielsen, A.L. Flores-Mireles, A.L. Kau, K.A. Kline, J.S. Pinkner, F. Neiers, S. Normark,
980 B. Henriques-Normark, M.G. Caparon, and S.J. Hultgren, Pilin and sortase residues critical
981 for endocarditis- and biofilm-associated pilus biogenesis in *Enterococcus faecalis*. *Journal of*
982 *bacteriology* 195 (2013) 4484-95.

983 [114] Q. Ma, Y. Zhai, J.C. Schneider, T.M. Ramseier, and M.H. Saier, Jr., Protein secretion systems
984 of *Pseudomonas aeruginosa* and *P fluorescens*. *Biochimica et biophysica acta* 1611 (2003)
985 223-33.

986 [115] D. Tielker, S. Hacker, R. Loris, M. Strathmann, J. Wingender, S. Wilhelm, F. Rosenau, and
987 K.E. Jaeger, *Pseudomonas aeruginosa* lectin LecB is located in the outer membrane and is
988 involved in biofilm formation. *Microbiology* 151 (2005) 1313-1323.

989 [116] E.K. Cassin, and B.S. Tseng, Pushing beyond the envelope: the potential roles of OprF in
990 *Pseudomonas aeruginosa* biofilm formation and pathogenicity. *Journal of bacteriology*
991 (2019).

992 [117] A. Li, P.Y. Lee, B. Ho, J.L. Ding, and C.T. Lim, Atomic force microscopy study of the
993 antimicrobial action of Sushi peptides on Gram negative bacteria. *Biochimica et biophysica*
994 *acta* 1768 (2007) 411-8.

995 [118] S.R. Schooling, A. Hubley, and T.J. Beveridge, Interactions of DNA with biofilm-derived
996 membrane vesicles. *Journal of bacteriology* 191 (2009) 4097-102.

997 [119] K.M.R. Parducho, Airway Peptides and Lipids- Effects on *Pseudomonas aeruginosa*
998 Morphology, Biofilm Formation, and Quorum Sensing, Chemistry & Biochemistry,
999 California State University Los Angeles, Los Angeles, 2018.

1000 [120] J. Kyte, and R.F. Doolittle, A simple method for displaying the hydropathic character of a
1001 protein. *Journal of molecular biology* 157 (1982) 105-32.

1002 [121] W.C. Wimley, and S.H. White, Experimentally determined hydrophobicity scale for proteins at
1003 membrane interfaces. *Nature structural biology* 3 (1996) 842-8.

1004

1005 **Tables**1006 **Table 1.** Human Beta Defensins-2 and -3 physicochemical properties.

Peptide	Amino acid sequence ^a	MW (Da)	Net Charge	Hydrophobicity index	
				Kyte- Doolittle ^b	Wimley- White ^c
HBD2	GIGDPVTC¹LKSGAIC²HPVFC³P RRY KQIGTC ² GLPGTKC ¹ C ³ KKP	4,328.22	6	-0.1	6.16
Linear HBD2	GIGDPVTALKSGAIHPVFA P ^{RRYK} QIGTAGLPGTKA AK KKP	4,141.88	6	-0.21	8.62
HBD3	GIINTLQKYYC ¹ RVRGGRC²AVLSC³ LPKEEQIGKC ² STRGRKC ¹ C ³ RRKK	5,155.19	11	-0.7	12.65

^a Amino acid sequences are given in one-letter code starting from the N and ending with the C terminus. Underlined residues denote mutation sites for the linearized HBD2. Cationic residues are in boldface. Anionic residues are italicized.

^b Values were calculated based on the Kyte-Doolittle hydrophobicity scale [120] using the grand average of hydropathy (GRAVY) program. Higher values represent an increase in hydrophobicity.

^c Values were calculated based on the Wimley-White whole residue hydrophobicity interface scale (Wimley & White 1996) [121] using the APD3 antimicrobial peptide calculator and predictor. Lower values represent an increase in hydrophobicity.

¹⁻³ Numbers denote disulfide bond connectivity.

1007
1008
1009
1010
1011
1012
1013
1014
1015

1016

1017

Table 2. Primers used in this study.

Gene target		5' - 3' Sequence	T _M (°C)	Product size (bp)	Product melt peak (°C)
<i>pslA</i>	F	CGTTCTGCCTGCTGTTGTT	56.9	160	88.5
	R	TACATGCCCGCGTTTCATCCA	57.3		
<i>gapA</i>	F	CCATCGGATCGTCTCGAA	61.0	130	88.0
	R	GTTCTGGTCGTTGGTAG	60.0		
<i>flgF</i>	F	ACAAACCTGGCGAACATCTC	62.0	137	89.0
	R	GCCATGGCTGAAATCGGTA	62.0		

1018

1019 **Table 3.** Dissociation constants for quorum sensing molecules calculated using AutoDock Vina
 1020 measurements. The best binding energies (predicted by AutoDock Vina) for each ligand-receptor pair
 1021 were used to manually calculate dissociation constants (K_D) using Equation [1]. NEtP:
 1022 phosphorylcolamine; 3-oxo-C12-HSL: N-(3-oxododecanoyl) homoserine lactone; C4-HSL: N-
 1023 butanoyl homoserine lactone; PQS: 2-heptyl-3-hydroxy-4-quinolone.
 1024

Receptor	NEtP	3-oxo-C12--HSL	C4-HSL	PQS _t
LasR	558 μ M	1.15 μ M	18.3 μ M	191 nM
HBD2	4.637 mM	3.348 mM	2.417 mM	403 μ M

1025

1026

1027 **Figure Legends**1028 **Figure 1**

1029 **Metabolic activity of *P. aeruginosa* in the presence and absence of HBD2 and HBD3 over 18 h.**
1030 Bacteria were incubated in 10% Mueller-Hinton/140 mM NaCl supplemented with 0.01 % resazurin
1031 and fluorescence emitted by resorufin reflecting the production of reducing metabolites was
1032 measured every 3 h (530 nm_{ex}, 616 nm_{em}). Shown are the means \pm SD of three independent
1033 experiments conducted in duplicates. RFU: relative fluorescence units. $p < 0.001$ for HBD2 (A) at 1,
1034 2, and 4 μ M and for HBD3 (B) at 0.25, 0.5, and 1 μ M compared to the solvent control in univariate
1035 ANOVA with Bonferroni posthoc analysis. All other concentrations were not significantly different
1036 from the solvent controls.

1037

1038 **Figure 2**

1039 **Comparative effects of HBD2 and HBD3 on *P. aeruginosa* biofilm and metabolic activity.**
1040 Shown are biofilm formation and accumulated resorufin fluorescence after 18 h of incubation with
1041 HBD2 (A) and HBD3 (B) at the concentrations given. Data are expressed relative to the control and
1042 represent means \pm SD of three independent experiments conducted in triplicates. *** $p = 0.0004$ in
1043 Two-way ANOVA. N.S: not significant ($p = 0.7721$).

1044

1045 **Figure 3**

1046 **ATP quantification in *P. aeruginosa* after 18 h incubation in the presence or absence of HBD2**
1047 **and HBD3 at the concentrations given.** ATP concentrations are in nM and were calculated based
1048 on a standard curve. Shown are means \pm SD of three independent experiments conducted in
1049 duplicates. $p = 0.01$ in One way ANOVA with Bonferroni posthoc analysis for 2 μ M HBD2
1050 compared to 2 μ M HBD3.

1051

1052 **Figure 4**

1053 **Effects of HBD2 on *A. baumannii* biofilm formation and metabolic activity.** Shown are crystal
1054 violet absorbance and accumulated resorufin fluorescence expressed as % of the control after 18 h of
1055 incubation with HBD2 at the concentrations given. Data represent means \pm SD of three independent
1056 experiments conducted in triplicates. ** $p = 0.004$ for biofilm reduction *versus* reduction of metabolic
1057 activity in two tailed Paired Samples Test. In Oneway ANOVA with Bonferroni posthoc analysis, p
1058 = 0.001 for resazurin reduction at 4 μ M HBD2, and $p < 0.001$ for biofilm reduction at 1, 2, and 4 μ M
1059 HBD2, compared to the solvent control. All other data points were not significantly different from
1060 the control.

1061

1062 **Figure 5**

1063 **Comparative effects of D- HBD2 and linear HBD2 on *P. aeruginosa* biofilm and metabolic**
1064 **activity.** Shown are biofilm formation and accumulated resorufin fluorescence expressed as % of the
1065 control after 18 h of incubation with all D- HBD2 (A) and linear HBD2 (B) at the concentrations
1066 given. Data represent means \pm SD of three independent experiments conducted in triplicates. In
1067 Paired T test comparing biofilm reduction and reduction of metabolic activity, *** $p < 0.001$ for D-
1068 HBD2 (A) and not significant (N.S.) for linear HBD2 (B). In Oneway ANOVA with Bonferroni
1069 posthoc analysis, biofilm formation ($p = 0.033$) but not metabolic activity ($p = 0.473$) is significantly
1070 reduced by D-HBD2. For linear HBD2, none of the data is significantly different from the solvent
1071 control.

1072

1073

1074 **Figure 6**

1075 **In silico docking and binding energies (ΔG) of various QS molecules calculated for LasR and**
 1076 **HBD2.** AutoDock Vina was used to predict binding sites and potential hits for HBD2 and quorum
 1077 sensing molecules in comparison to LasR. **(A)** Test *N*-(3-oxohexanoyl) homoserine lactone (3-oxo-
 1078 C12-HSL, green) lies inside the LasR binding pocket in the same region as co-crystallized 3-oxo-
 1079 C12-HSL (blue) with LasR (RSCB 3IX3). **(B)** HBD2 does not contain a binding pocket for test 3-
 1080 oxo-C12-HSL (green). Free energy of binding (ΔG) for various hits were determined for
 1081 phosphorylcolamine (NEtP), 3-oxo-C12-HSL, *N*-butyryl homoserine lactone (C4-HSL), and 2-
 1082 heptyl-3-hydroxy-4-quinolone (PQS) as ligands with either LasR **(C)** or HBD2 **(D)** as rigid receptors.
 1083 Dashed lines indicate the -6 kcal/mol threshold for actively bound molecules.
 1084

1085 **Figure 7**

1086 **Relative gene expression of *flgF* and *pslA* in the presence and absence of 0.25 μ M HBD2 as**
 1087 **determined by qPCR.** Gene expression of *flgF* **(A)** and *pslA* **(B)** in *P. aeruginosa* was calculated
 1088 relative to the reference gene *gapA* after incubation in the presence or absence of HBD2 for up to 12
 1089 h. Shown are means \pm SEM, n = 6. In multivariate ANOVA with Bonferroni posthoc analysis (${}^*p <$
 1090 0.05 and ${}^{**}p < 0.01$), gene expression of *flgF* and *pslA* changed over time (Control: $p < 0.01$ for *flgF*
 1091 0.5 h versus 6 h and 12h, and $p < 0.05$ for *pslA* 2 h versus 6 h and 12 h; HBD2: $p < 0.05$ for *flgF* 0.5
 1092 h versus 12 h) but there was no significant difference between the control and HBD2 treated
 1093 bacteria.

1094

1095

1096 **Figure 8**

1097 **Outer membrane protein profile of *P. aeruginosa* after 18 h incubation in the presence and**
 1098 **absence of HBD2.** **(A)** Four μ L of concentrated outer membrane preparations from HBD2 treated
 1099 (0.125 – 1 μ M) or solvent control exposed bacteria (0) were resolved by SDS Tris-Tricine PAGE and
 1100 visualized by silver stain. (Med) indicates medium only processed like bacteria-containing samples.
 1101 The band migrating between 10 and 15 kDa in all samples is consistent with the expected molecular
 1102 weight of lysozyme (14 kDa) that was added to the extraction buffer. **(B)** Approximate molecular
 1103 weight and intensities of bands were quantified with Image Lab software and band intensities
 1104 detected in both replicates were normalized to the intensity of the presumptive lysozyme band. Each
 1105 data point represents the average of replicates. Each line represents the protein profile for the
 1106 indicated HBD2 concentration (in μ M).

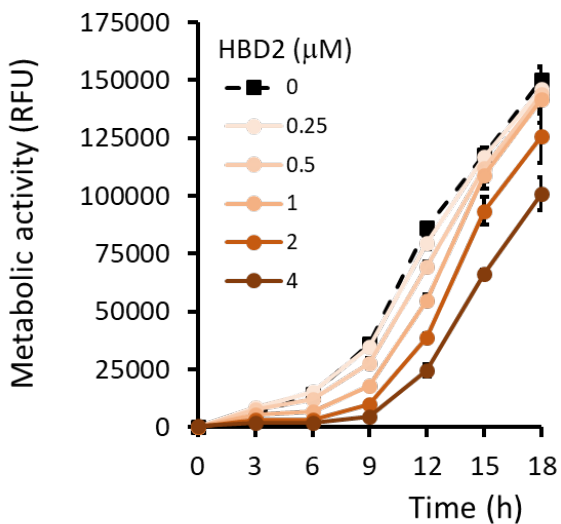
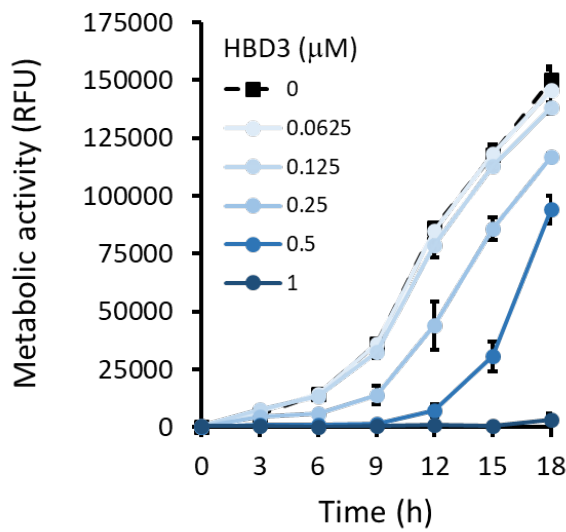
1107

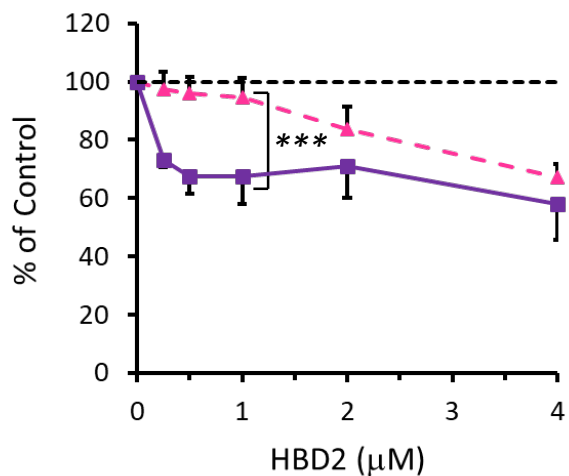
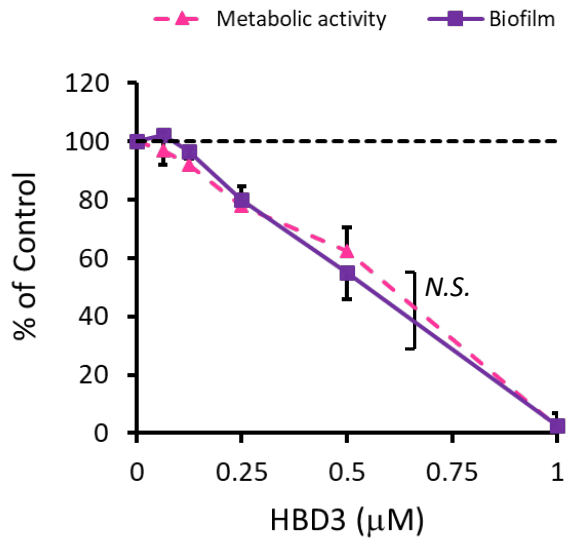
1108

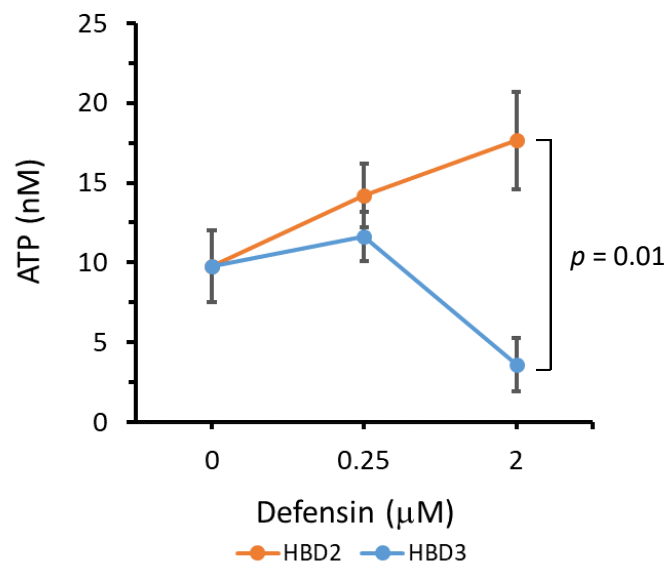
1109 **Figure 9**

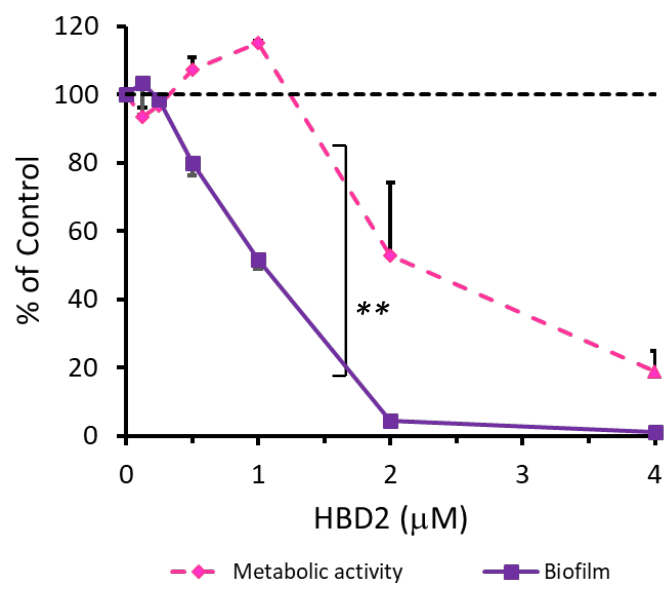
1110 **Atomic force microscopy of *P. aeruginosa* after 18 h incubation in the presence and absence of**
 1111 **0.25 μ M HBD2.** Bacteria were incubated on glass slides and fixed with 2.5 % glutaraldehyde prior to
 1112 imaging. Images taken with the atomic force microscope were first order flattened before extracting
 1113 measurement for bacterial roughness. **(A)** Representative images. CTRL: solvent control exposed
 1114 bacteria. **(B)** Box and whisker chart (with inner points and outliers) of roughness measurements from
 1115 multiple images of solvent exposed control bacteria (CTRL, n = 85) and 0.25 μ M HBD2 treated
 1116 bacteria (n = 69). ${}^{***}p < 0.001$ in independent samples T test.

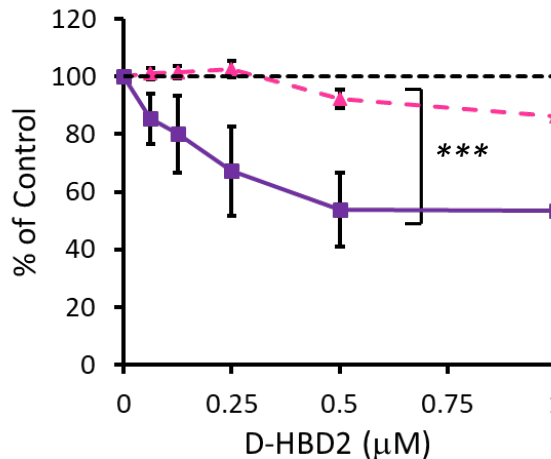
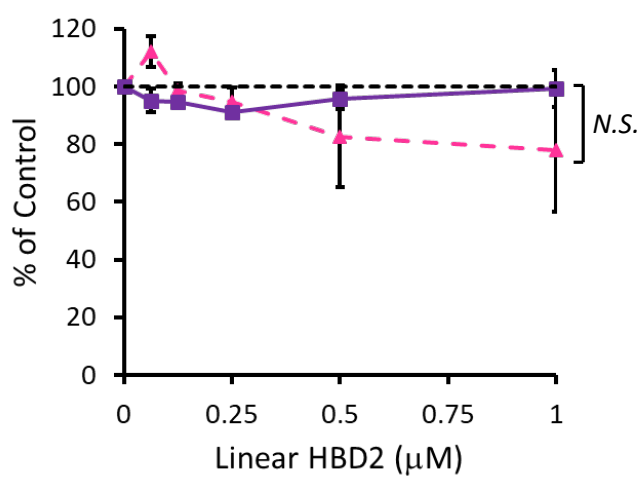
1117

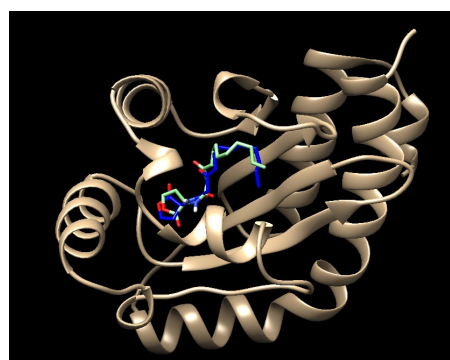
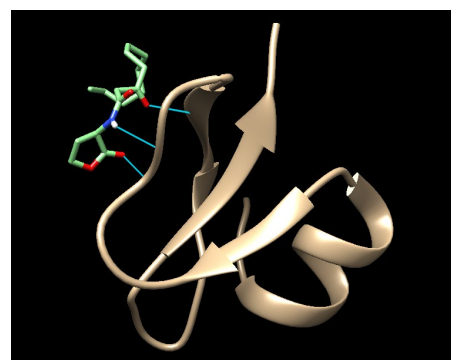
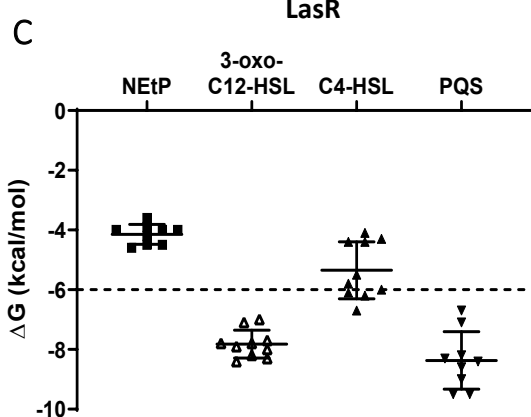
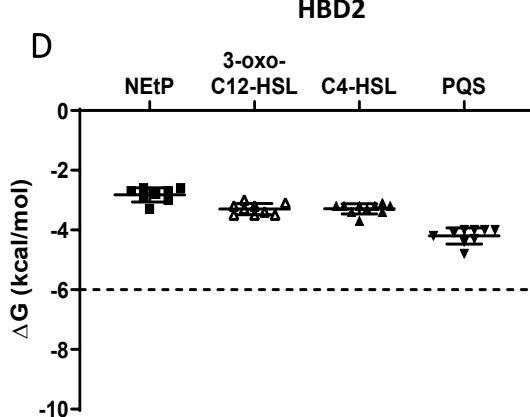
A**B**

A**B**

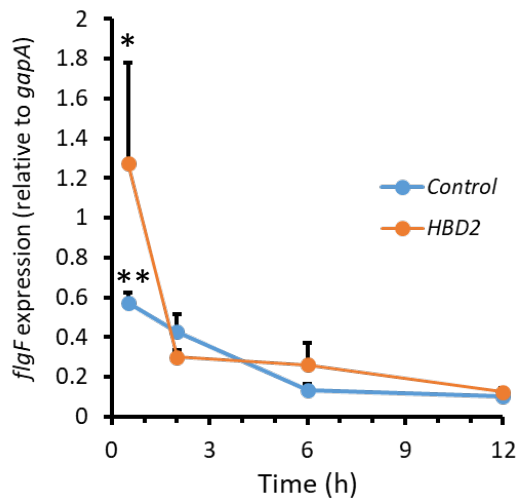




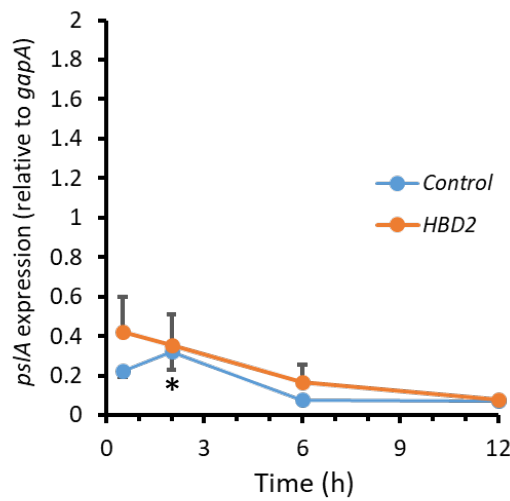
A**B**

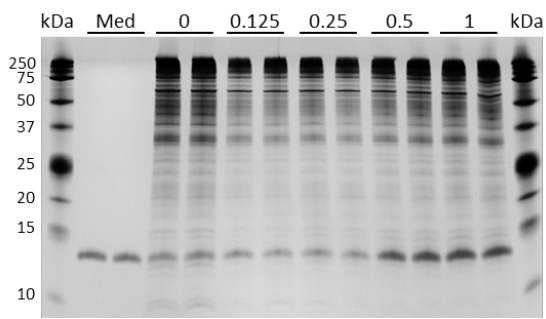
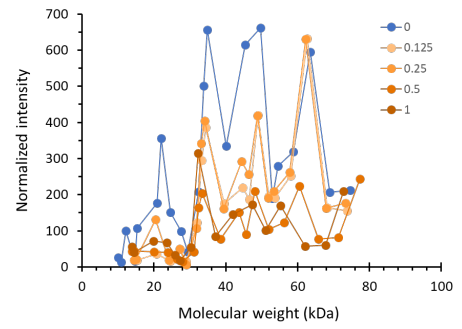
A**B****C****D**

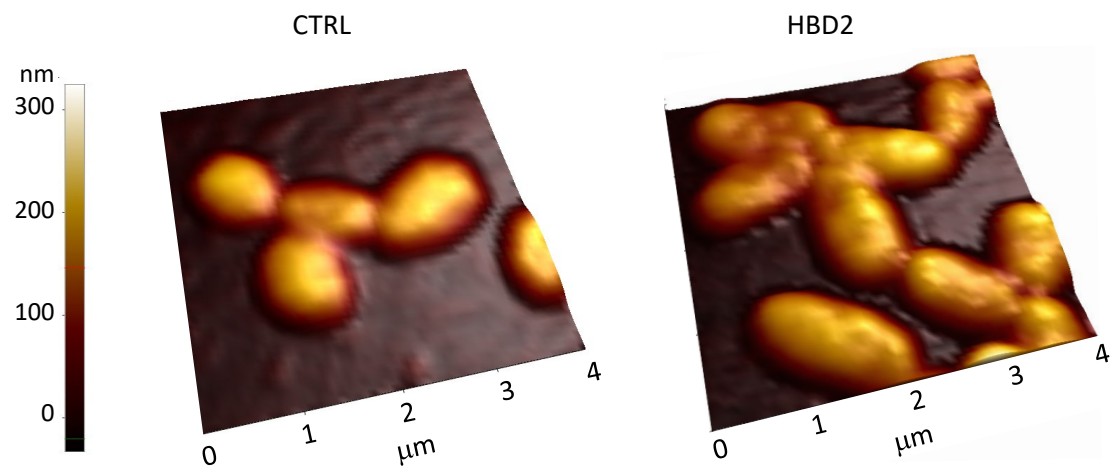
A



B



A**B**

A**B**